No. 3 1972

Technical Review

To Advance Techniques in Acoustical, Electrical and Mechanical Measurement

Noise and Vibration Transducers

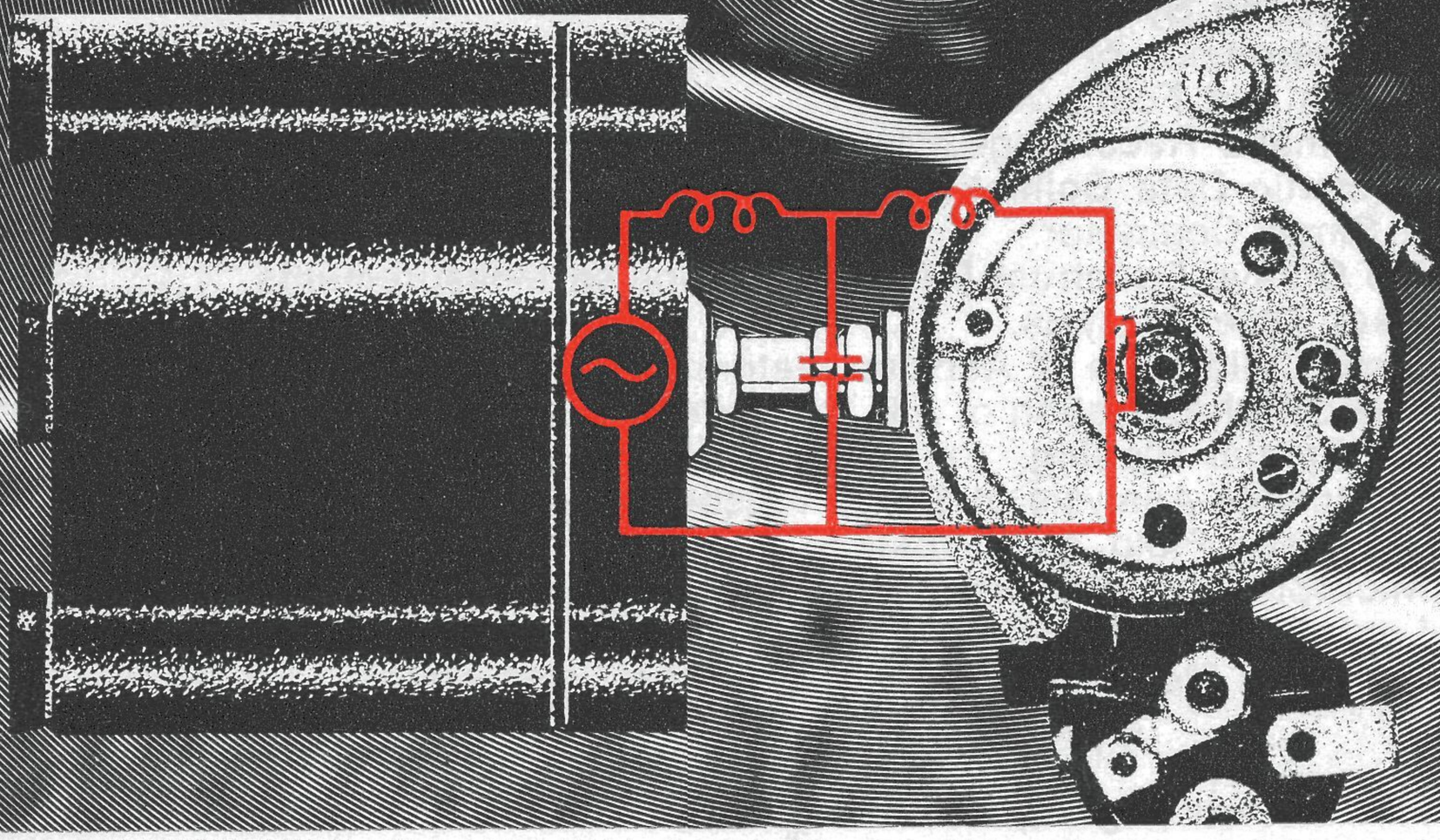

BRÜEL & KJÆR

PREVIOUSLY ISSUED NUMBERS OF BRÜEL & KJÆR TECHNICAL REVIEW

2–1972 RMS-Rectifiers.
Scandinavian Efforts to Standardize Acoustic Response in Theaters and Dubbing Rooms.
Noise Dose Measurements.

1–1972 Loudness Evaluation of Acoustic Impulses.
Computer Programming Requirements for Acoustic Measurements.
Computer Interface and Software for On-Line Evaluation of Noise Data.
Evaluation of Noise Measurements in Algol-60.

4–1971 Application of Electro-Acoustical Techniques to the Determination of the Modulus of Elasticity by a Non-Destructive Process.
Estimation of Sound Pressure Levels at a Distance from a Noise Source.
Acoustical Calibrator Type 4230 and its Equivalent Diagram.

3–1971 Conventional & On-line Methods of Sound Power Measurements.
An Experimental Channel Selector System.

2–1971 Interchangeable Head Vibration Exiters.
AEROS: A Generalized-Spectrum Vibration-Control System.

1–1971 Shock and Vibration Isolation of a Punch Press.
Vibration Measurement by a Laser Interferometer.
A portable Calibrator for Accelerometers.
Electro Acoustic Ear Impedance Indicator for Medical Diagnosis.

4–1970 On the Applicability and Limitations of the Cross-Correlation and Cross-Spectral Density Techniques.

3–1970 On the Frequency Analysis of Mechanical Shocks and Single Impulses.
Important Changes to the Telephone Transmission Measuring System.

2–1970 Measurement of the Complex Modulus of Elasticity of Fibres and Folios.
Automatic Recording-Control System.

1–1970 Acoustic Data Collection and Evaluation with the Aid of a Small Computer.
1/3 Octave Spectrum Readout of Impulse Measurements.

4–1969 Real Time Analysis.
Field Calibration of Accelerometers.
The Synchronization of a B & K Level Recorder Type 2305 for Spatial Plotting.

3–1969 Frequency Analysis of Single Pulses.

2–1969 The Free Field and Pressure Calibration of Condenser Microphones using Electrostatic Actuator.
Long Term Stability of Condenser Microphones.
The Free Field Calibration of a Sound Level Meter.

(Continued on cover page 3)

TECHNICAL REVIEW

No. 3 – 1972

Contents

Thermal Noise in Microphones and Preamplifiers

by

Viggo Tarnow

ABSTRACT

The smallest sound pressure that could be measured by condenser and piezoelectric microphones was in the past determined by the noise from their preamplifiers. However, the development of preamplifiers have reached a stage where their noise is less than the noise generated by the thermal vibrations of the membrane. This is shown experimentally by measuring the dependency of noise voltage on temperature. The experimental observation is compared with a computation of the noise voltage.

The noise sources in modern preamplifiers are discussed and the noise spectrum of the whole sound receiving system is given.

SOMMAIRE

La plus faible pression acoustique mesurable à l'aide de microphones électrostatiques ou piézoélectriques était, par le passé, fixée par le bruit engendré dans les préamplificateurs. Cependant, les développements des préamplificateurs ont été tels que leur bruit est maintenant inférieur au bruit engendré par les vibrations thermiques de la membrane.

Ce phénomène est montré expérimentalement en mesurant la relation entre la tension de bruit et la température. Les résultats expérimentaux sont comparés aux calculs de la tension de bruit.

On discute les sources de bruit des préamplificateurs modernes et on donne le spectre de bruit du récepteur acoustique global.

ZUSAMMENFASSUNG

Der kleinste Schalldruck, der mit einem Kondensator- oder Piezomikrofon gemessen werden konnte, war bisher durch das Rauschen der verwendeten Vorverstärker bestimmt. Die Entwicklung der Vorverstärker hat jetzt jedoch ein Stadium erreicht, wo deren Eigenrauschen geringer ist als das Rauschen, das durch thermische Bewegung der Membran hervorgerufen wird.

Dies wird experimentell durch Messung der Abhängigkeit der Rauschspannung von der Temperatur nachgewiesen. Das Ergebnis wird schließlich mit einer Berechnung der Rauschspannung verglichen.

Die Rauschquellen in modernen Vorverstärkern werden diskutiert, und das Rauschspektrum des gesamten Schall-Empfangssystems wird erläutert.

Introduction

In a well designed sound receiving system with condenser or piezoelectric microphones there are two important sources of thermal noise which limit the ultimate performance of the system. The first is noise from the microphone generated by the Brownian movements of the membrane. The second is electronically generated noise in the preamplifier associated with the microphone.

A typical sound measuring system consists of a microphone, a preamplifier, an amplifier and a detector with a meter on which a root mean square voltage can be read. The frequency response of the electronic system is often complicated and different responses are used.

Therefore it is most instructive to consider noise sources in terms of the noise spectra. From the spectra the output noise voltage of a system may be computed, when its frequency response is known.

In the first part of this paper the noise spectra and noise voltages of the microphones are computed. In the second part a measurement of the noise voltage is described and in the third part the noise from the preamplifiers is computed and the noise from microphones and preamplifier is added.

Computation of Noise Voltage from Microphones

Information about the output voltage from a microphone due to Brownian movements of its membrane is desired. What may be computed are the two statistical quantities, the spectral density and the mean square voltage. These may be found from the corresponding values for the deflection of the membrane.

The membrane of the condenser microphone is a mechanical system with many degrees of freedom. However, it is sufficiently accurate to use only one degree of freedom for the present case.

The generalized space coordinate is taken to be equal to the volume displacement which is equal to the integral of the deflection of the membrane over the surface of the membrane. The generalized momentum associated with this volume displacement is equal to the pressure.

In the paper by H.B. Callen and T.R. Welton (1951) ref. 1, it is shown that the statistical properties of the dynamic system may be computed by using a generalized Nyquist formula. It is assumed that a pressure with mean square value, $\Delta\overline{p^2}$ given in formula (1), is applied to the membrane.

$$\Delta\overline{p^2} = 4\,kT\,Re\,[Z]\,\Delta f \qquad (1)$$

where
- k is the Boltzmann constant
- T is the absolute temperature
- Δf is the frequency bandwidth
- Z is the acoustic impedance of the membrane defined in formula (2)

If the volume displacement is v and the pressure p one has

$$p = Z(\omega)\, i\omega v \tag{2}$$

The spectral density of the volume displacement may be obtained from formulas (1) and (2):

$$\overline{\Delta v^2} = 4\,kT\,\frac{\mathrm{Re}\,[Z(\omega)]}{\omega^2\,|Z(\omega)|^2}\Delta f \tag{3}$$

The mean square value of the volume displacement is found by using a statistical mechanics law which states that the mean value of the potential energy of a harmonic oscillator equals 1/2 kT. The stiffness, s, is introduced by

$$s = \lim_{\omega \to 0} i\omega Z(\omega) \tag{4}$$

It may be shown that s is real, see ref. 2.

The mean potential energy equals $1/2\,\overline{sv^2} = 1/2\,kT$, from which the following is obtained

$$\overline{v^2} = kT/s \tag{5}$$

This could be obtained from formula (3) by integrating the expression over all frequencies. This is shown in L.P. Landau and E.M. Lifschitz, ref. 2.

The open circuit voltage of the microphone is proportional to the volume displacement, that is

$$e = cv \tag{6}$$

where the constant, c, is independent of frequency. It is related to the pressure sensitivity, $F(\omega)$ defined by*)

$$e = F(\omega)\, p \tag{7}$$

---

* $F(\omega)$ is known from the measurements of the microphone pressure sensitivity with the electrostatic actuator. With this a constant pressure across the membrane is obtained by an electrostatic field.

By substituting the expression (2) for p in (7) and comparing it with (6) one obtains

$$c = F(\omega)\, i\omega Z(\omega) \tag{8}$$

but c does not depend on frequency and, therefore, using expression (4)

$$c = F(0)\, s \tag{9}$$

From formulas (3), (6) and (8) one obtains the spectrum for the output voltage

$$\Delta\overline{e^2} = |F(\omega)|^2\, 4\,kT\, Re\,[Z(\omega)]\,\Delta f \tag{10}$$

By taking the mean square of both sides of formula (6) we have

$$\overline{e^2} = c^2 \cdot \overline{v^2} \tag{11}$$

By inserting formulas (3) and (9) in (11) we obtain

$$\overline{e^2} = F^2(0)\, skT \tag{12}$$

In the following it is assumed that the acoustic impedance has the form

$$Z(\omega) = (s + i\omega r - m\omega^2)/i\omega \tag{13}$$

where the parameters r and m are independent of frequency.

The noise voltages and pressures for some Brüel & Kjær microphones are shown in table 1. The values of sensitivity, stiffness and resistance have been obtained from the instruction manuals. The stiffnesses and resistances are directly given in the manuals for the microphones types 4144, 4145 and 4134. For the other condenser microphones the stiffness values have been estimated from the equivalent volumes given in the manuals. The parameters for the piezoelectric microphone Type 4117 were given by K. Styhr Hansen (1968), ref. 3.

The noise voltage e_n in table 1, should be used when a wide band amplifier is used. The noise voltage e_A has been obtained by assuming that the frequency response is of type A, which is recommended by various standards.

The amplification is taken to be 1 at 1000 Hz. The pressures given in table 1 have been obtained from the voltage by division by the sensitivity of the microphones.

Microphone	Sensitivity F	Stiffness s	Resistance r	Voltage e_n	Pressure $p_n = e_n/F$	Voltage e_A	Pressure $p_A = e_A/F$
	10^{-3} V/(dyn/cm^2)	10^6 dyn/cm^5	dynsec/cm^5	10^{-6} Volt	10^{-4} dyn/cm^2	10^{-6} Volt	10^{-4} dyn/cm^2
4144 1 inch	5	10.4	180	3.3	6.6	3.3	6.6
4145 1 inch	5	11.1	447	3.3	6.6	3.3	6.6
4133 1/2 inch	1.25	170	3030	3.3	26	2.5	20
4134 1/2 inch	1.25	170	1540	3.3	26	2.4	19
4148 1/2 inch	1.25	21	640	1.2	9.3	1.2	9.6
4177 piezoelec.	0.3	4.6	257	0.13	4.3	0.13	4.2

Tabel 1.

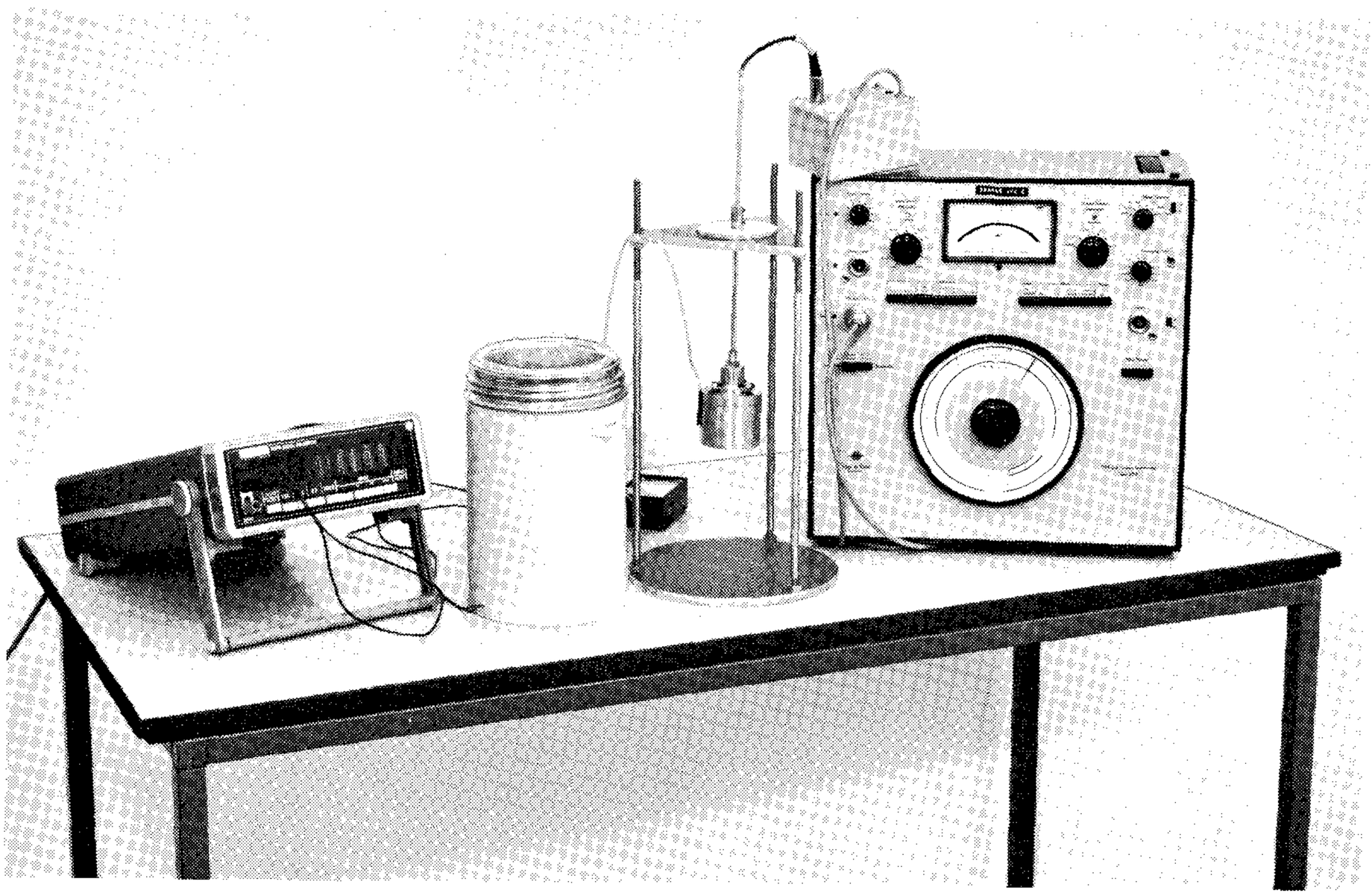

Fig. 1. The experimental arrangement for measuring the thermal noise from microphones. In the centre of the picture the brass cylinder containing the microphone hangs in a thin steel tube. Through the tube a cable is drawn which connects the condenser microphone to the preamplifier. The preamplifier is connected to the spectral analyzer at the right of the picture. When noise is measured the Dewar vessel is filled with liquid Nitrogen and the cylinder is placed in the Dewar. The temperature of the cylinder is read on the instrument to the left, which is connected to a platinum resistor placed on the brass cylinder.

Measurements of the Noise from Microphones

The noise voltage from preamplifiers are at present so low that noise from microphones should be considered. This is shown experimentally by measuring the noise voltage from a one inch condenser microphone. The microphone was mounted in a thick-walled brass cylinder, which was sealed airtight. The experimental set-up is shown on Fig.1. The microphone was connected via a preamplifier to a spectrum analyzer from which a root mean square output voltage was obtained. The brass cylinder was cooled by means of liquid nitrogen in a Dewar vessel. The temperature of the microphone was measured with a Platinum resistance thermometer and the preamplifier was kept at a constant temperature. With this arrangement the noise voltage was measured as a function of temperature as presented in Fig.2.

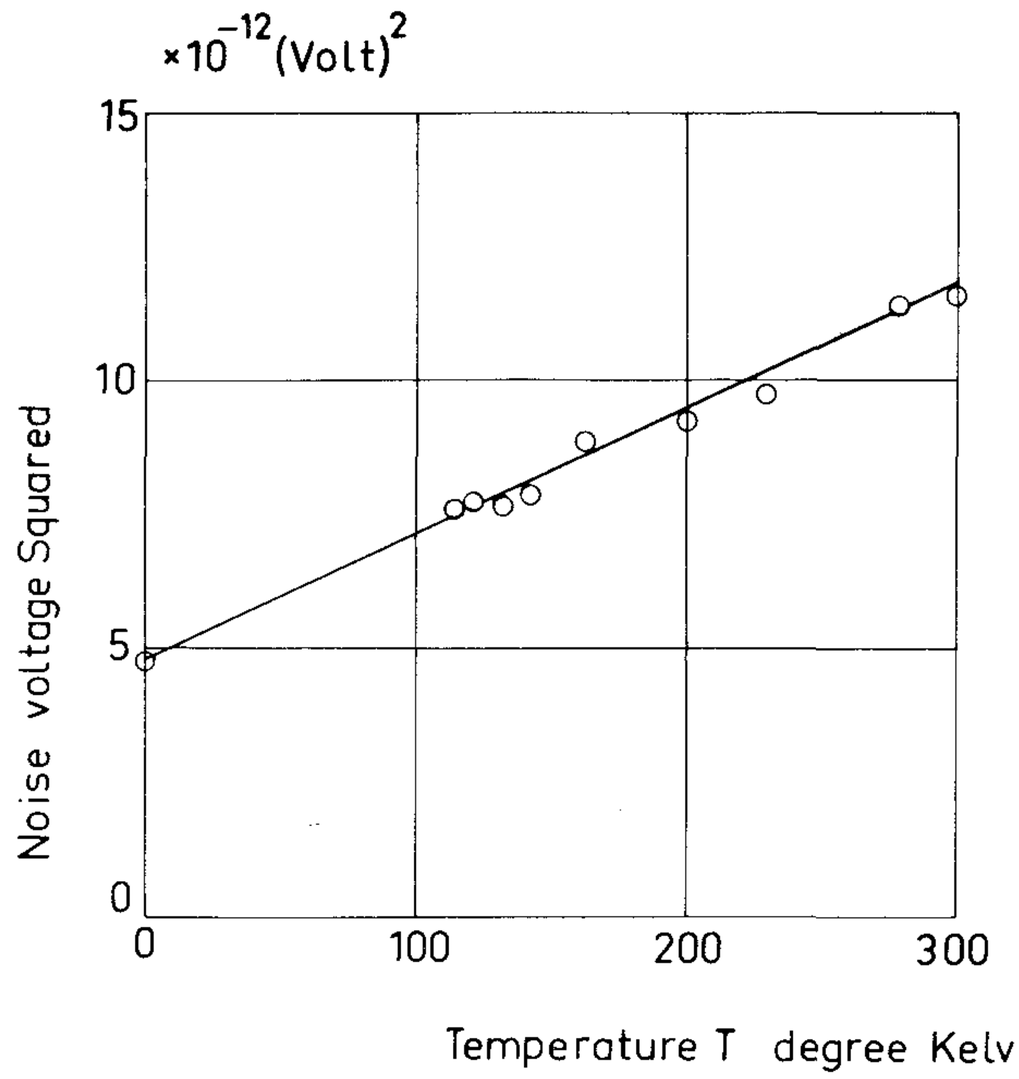

Fig.2. The variation of the mean square noise voltage with temperature. The plotted points in the figure are obtained from the observed voltages divided by a factor equal to the amplification of the open circuit voltages from the microphone. The squared voltages are the sums of the squared voltages of readings from 1/3 octave filters. The filters used covered the frequency range from 400 to 20.000 Hz, but a correction has been made in order to extrapolate to a frequency range from 0 to 20.000 Hz. The ordinate at the point at 0 degree absolute temperature was measured by replacing the microphone by a capacitor which had the same capacitance as the microphone. This point represents the electronic noise voltage from the preamplifier

The noise from the preamplifier does not depend on the temperature of the microphone. Therefore the temperature variation of noise voltage is due to microphone noise alone and the noise voltage curve shows the temperature variation to be expected from thermally generated vibrations of the diaphragm.

From Fig.2 it is easy to find the measured root mean square voltage due to thermal vibrations, it is 2,7 μV at 27°C. (The value is the open circuit voltage of the microphone). The computed value for the used microphone was 2,9 μV.

The frequency spectrum of the noise from the microphone is shown in Fig.3. The square of the noise voltage from the electronic system has been subtracted. The variation with frequency is similar to the variation of the sensitivity, within the experimental errors. This would be expected from the theoretical considerations above.

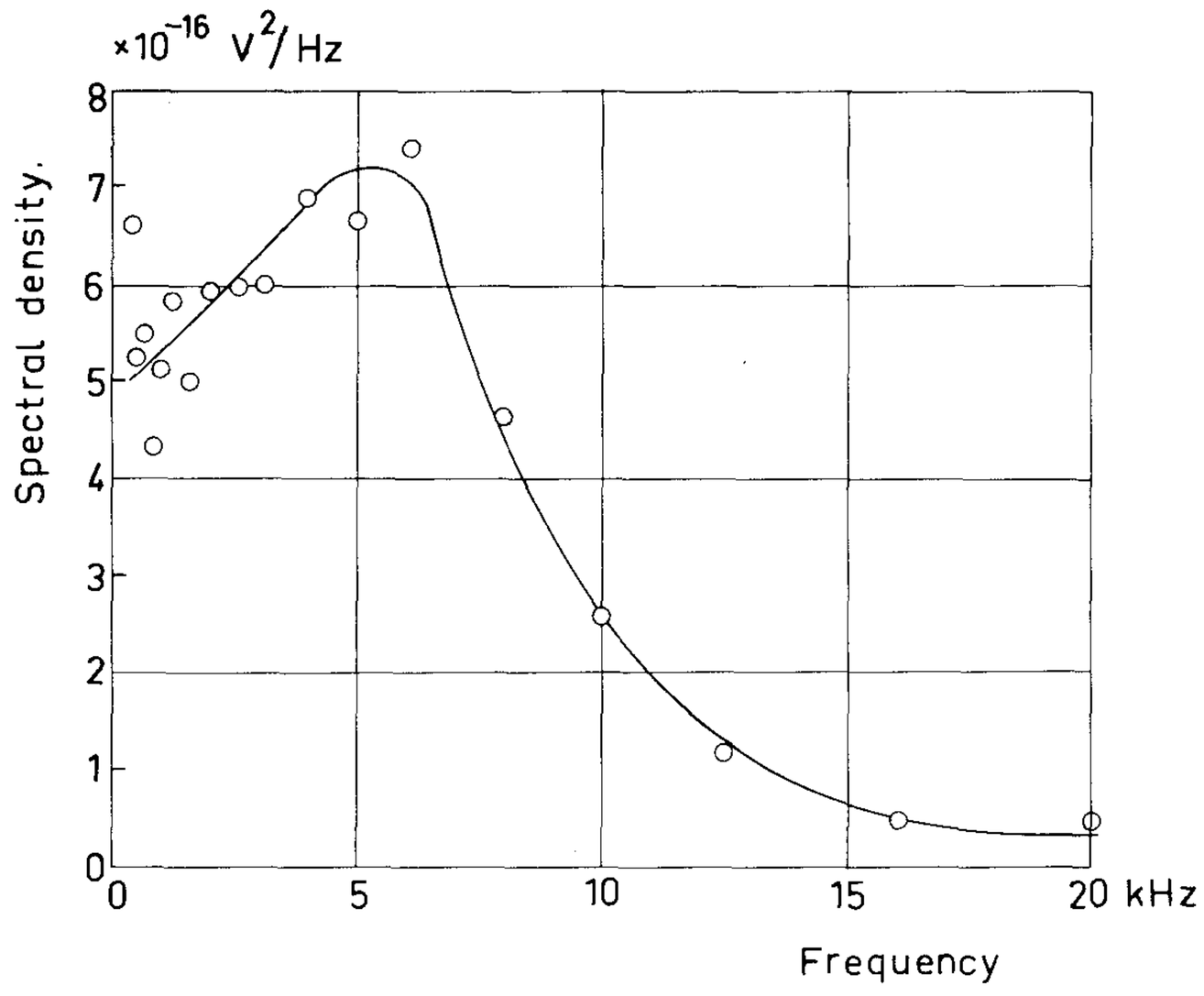

Fig.3. Frequency spectrum of thermal noise from a one inch condenser microphone Type 4144. Given is the mean square of the open circuit voltage. The nominal polarization voltage was used

Noise of preamplifiers and microphones

An idealized preamplifier circuit is shown in Fig.4. The amplifier incorporates a junction field effect transistor. If the whole measuring system is well designed, noise from the source resistor and the noise from the amplifier

following the preamplifier may be neglected. The input capacitance of the preamplifier is disregarded in the following discussion, and the voltage amplification of the preamplifier is taken to be 1.

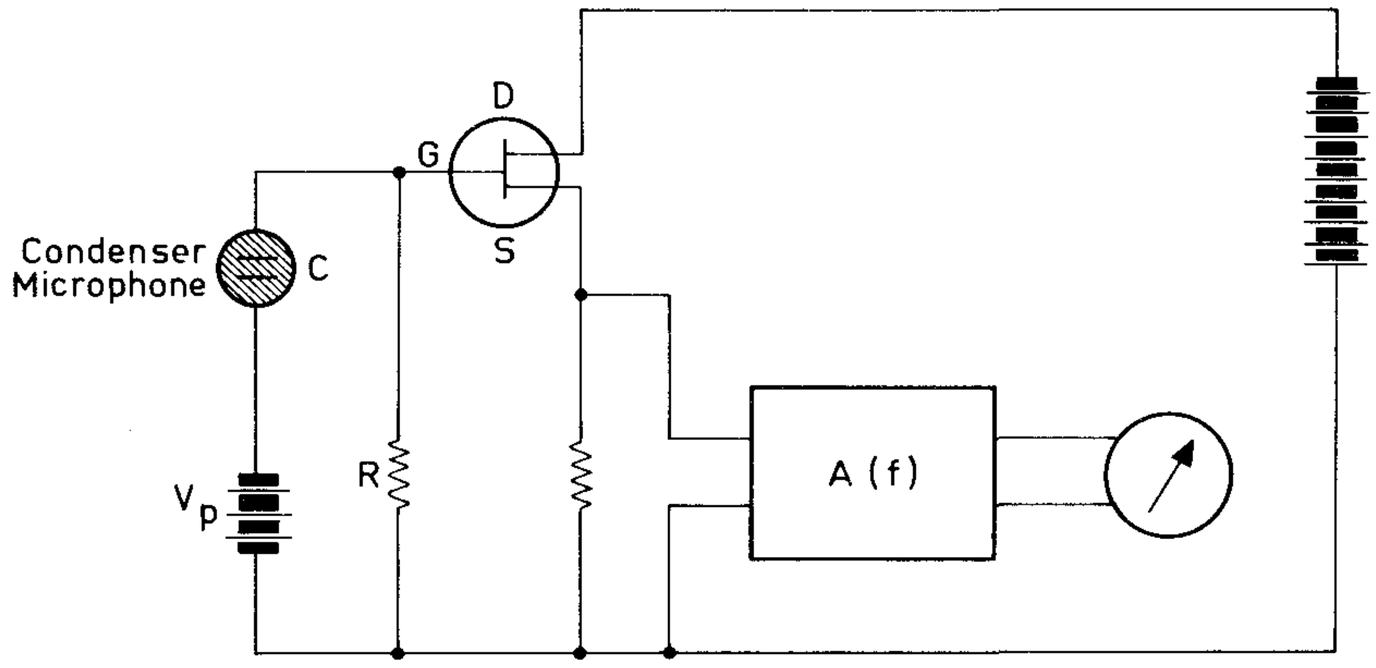

Fig.4. Simplified sketch of the preamplifier circuit

There are four main noise sources. Nyquist noise from the resistor in the gate circuit, shot noise from the gate current, noise from the channel of the field effect transistor, and "1/f" noise from the transistor.

In the frequency range of interest the noise output voltage may be computed from the following formula, given by R.S.C. Cobbold ref.4.

$$\overline{\Delta V^2} = \left[\frac{1}{C^2\omega^2}\,\frac{4\,kT}{R} + \frac{1}{C^2\omega^2}\;2\,q\,J_G + \frac{0.65}{g_m}\,4\,kT + \frac{A^2}{f}\right]\;\Delta f \qquad (14)$$

where
- C is the capacitance of the transducer
- ω is the cyclic frequency
- R is the gate resistor
- q is the electronic charge
- J_g is the gate leakage current
- g_m is the conductance of the transistor
- A is a constant for the value of the 1/f noise
- Δf is the frequency bandwidth

In order to minimize the shot noise it is important to have a small value of the gate current. The gate resistor should be as large as possible. Its magnitude is limited by the gate current because it is necessary to have a small voltage drop across the gate resistor, and the gate current depends strongly on temperature.

The following figures are used $i_{gs} = 2 \cdot 10^{-12}$A, R = 10^{10}ohm. The last two terms, in (14), were obtained from information given by a transistor manufacturer.

The noise voltage spectral density from the preamplifier is given in Figs.5, 6 and 7. The curves were computed from the formula above. The mean square output voltage from the measurement system may be found from

$$V^2 = \int_0^\infty A^2(f)\, v_f^2\, df \qquad (15)$$

where A(f) is the voltage amplification of the amplifier and v_f^2 the squared noise voltage density at the input. The ability of the system to detect small sound pressures is not changed when A(f) is multiplied by a constant factor, because the signal and the noise are amplified by the same factor; and the amplification is, therefore, taken to be 1 at 1000 Hz.

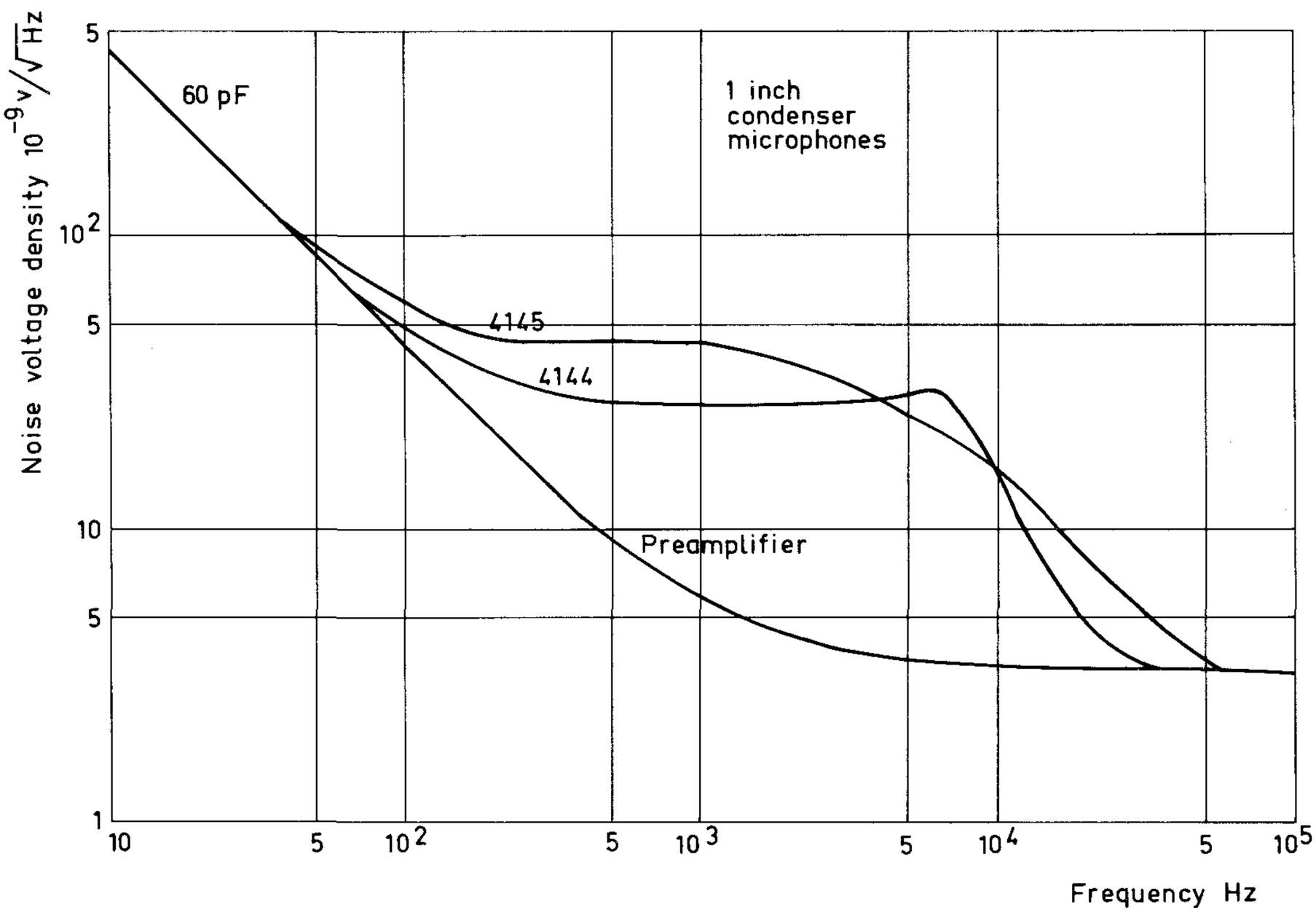

Fig.5. The noise voltage spectral density for one inch condenser microphones and the preamplifier. The upper curves present the noise of the whole system, and the lowest curve the noise of the preamplifier alone

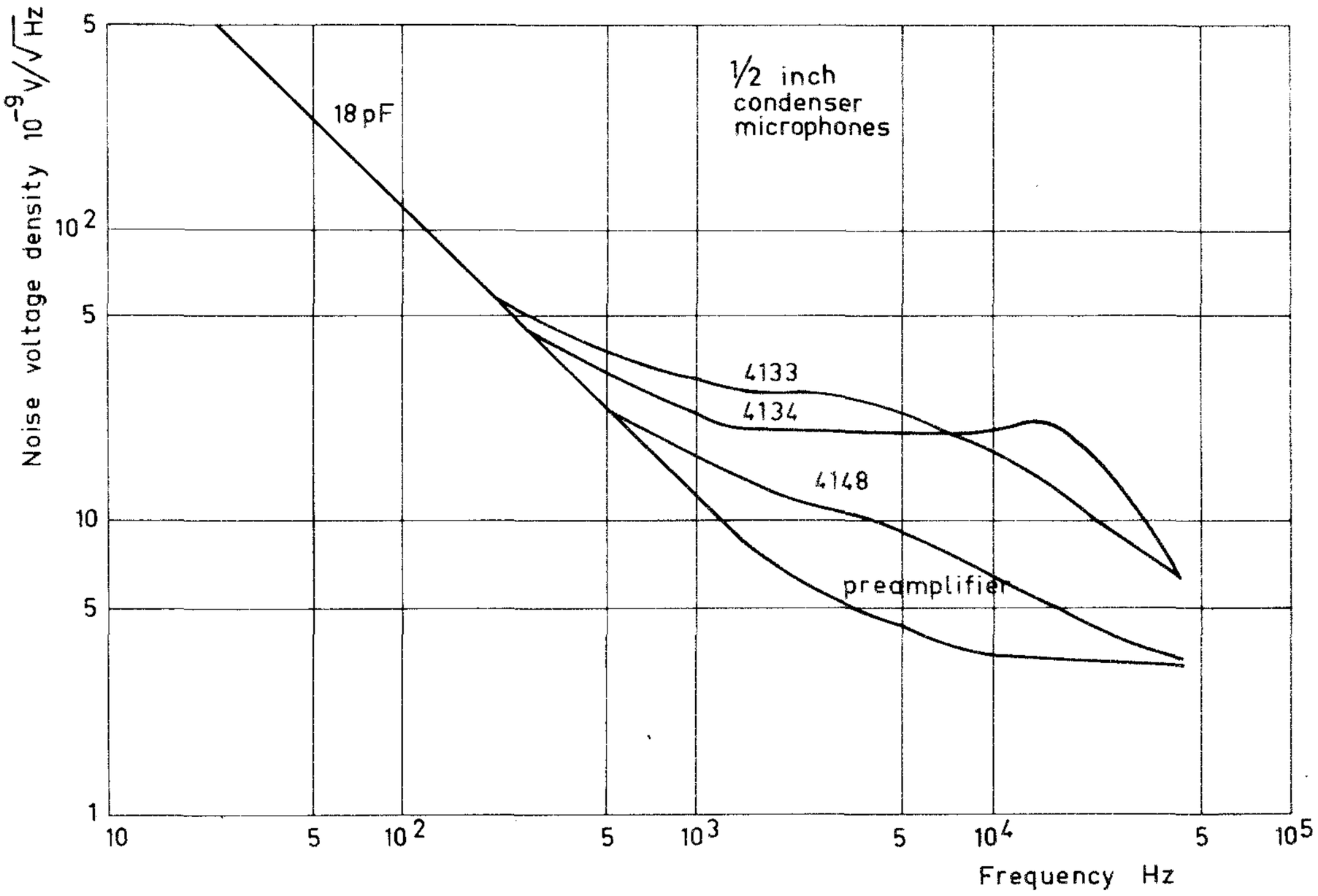

Fig.6. The noise voltage spectral density for half inch condenser microphones and the preamplifier. The lowest curve presents the noise of the preamplifier alone

The relative importance of the different noise sources may be estimated from a numerical example of the computation of the mean square noise voltage

$$\overline{\Delta V^2} = (51.7 \cdot 10^{-14} + 21.5 \cdot 10^{-14} + 18 \cdot 10^{-14} + 2.7 \cdot 10^{-14}) \text{ (Volt)}^2 \quad (16)$$

the terms are written in the same order as in the formula above. The capacity of the microphone is C = 60 pF, the frequency response is taken to be constant from 20 Hz to 20.000 Hz, outside this interval it is zero.

The noise voltages from the preamplifier with different microphones are shown in table 2. The wide band frequency response is from 20 Hz to 20.000 Hz for the microphones Types 4144, 4145 and 4117 and from 20 Hz to 200.000 Hz for Types 4133, 4134 and 4148. There is only a small change in noise voltage from the preamplifier when changing from the small bandwidth to the large. The shift in noise voltage is from 2,9 μV to 3,2 μV with a 18 pF microphone capacitance.

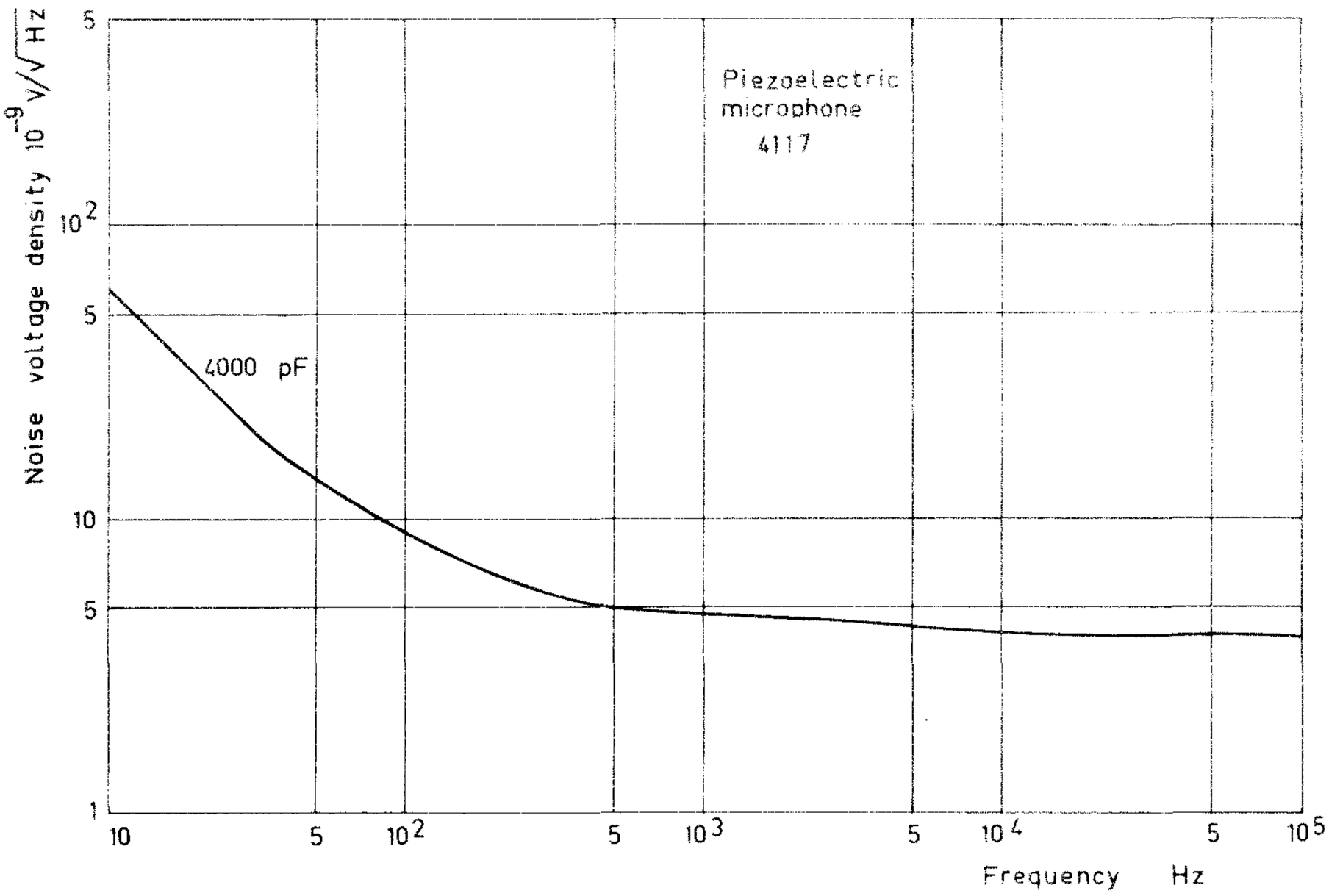

Fig.7. The noise voltage spectral density for the preamplifier with the piezoelectric microphone. The noise from the microphone may be neglected

Microphone	Capacity	Wide band frequency response			Type A frequency response		
		Preamplifier	Preamplifier and Microphone	Total noise pressure	Preamplifier	Preamplifier and microphone	Total noise pressure
	pF	10^{-6} Volt	10^{-6} Volt	10^{-4} dyn/cm^2	10^{-6} Volt	10^{-6} Volt	10^{-4} dyn/cm^2
4144	60	1.0	3.4	6.8	0.3	3.3	6.8
4145	60	1.0	3.4	6.8	0.3	3.3	6.8
4133	18	3.2	4.6	37	0.3	2.5	20
4134	18	3.2	4.6	37	0.3	2.4	19
4148	18	3.2	3.4	27	0.3	1.2	10
4117	4000	0.5	0.5	16	0.3	0.3	10

Tabel 2.

The voltage with curve A response was obtained by carrying out the integration implied in equation (15). With the type A response the capacitance of the microphone have no influence on the noise, but this is the case when low frequencies are used. The noise pressures have been obtained by dividing, the noise voltage from the preamplifier, with microphone mounted, by the pressure sensitivity of the microphone.

It is apparent from table 2 that the most important noise source in an optimal sound detecting system is the microphone. The lowest sound pressure that may be measured depends on the magnitude of error which can be accepted. If a relatively large error can be tolerated the lowest sound pressure is the one where noise voltage is equal to the voltage from the sound pressure to be measured.

In this case the smallest sound pressure, that may be detected is 11 dB re $2 \cdot 10^{-4}$ dyn/cm^2 in the frequency range 20 – 20.000 Hz. If the signal has a much smaller bandwidth than 20 – 20.000 Hz it is possible to measure smaller sound pressures. The smallest mean square pressure spectral densities that may be measured with filters can be estimated from the figures 5, 6, 7 which display the noise spectra for the whole measuring system.

References:

1. H.B. CALLEN and T.A. WELTON — Irreversibility and Generalized Noise Phys. Rev. 83, 34 (1951)

2. L.D. LANDAU and E.M. LIFSCHITZ — Statistische Physik, § 126, § 127 Akademie Verlag, Berlin. 1966

3. K. STYHR HANSEN — Details in the Construction of a Piezoelectric Microphone. The 6th International Congress on Acoustics. Tokyo, Japan, Aug. 21 – 28, 1968.

4. R.S.C. COBBOLD — Theory and Applications of Field-Effect Transistors, Chapter 9, 1970, John Wiley and Sons, Inc.

High-Frequency-Response of Force-Transducers

by

Willy Brænder

ABSTRACT

The paper describes the derivation of high frequency response of force transducers which depend on the transducer stiffness and its seismic masses as well as the mechanical impedances to which it is connected. The types of set-ups in which the transducer is used are also discussed, since they influence its frequency characteristics.

SOMMAIRE

Cet article décrit le calcul de la réponse haute-fréquence des capteurs de force, qui dépend de la raideur du capteur et de ses masses sismiques aussi bien que des impédances mécaniques auxquelles il est relié. Les différents types de montage où on utilise un capteur de force sont également discutés, puisqu'ils ont une influence sur ses caractéristiques en fréquence.

ZUSAMMENFASSUNG

In dem Artikel wird die Herkunft der Resonanzspitzen im Frequenzgang von Kraftaufnehmern bei höheren Frequenzen beschrieben. Deren Abhängigkeit von der Steifigkeit und der seismischen Masse des Aufnehmers und des Prüflings sowie von der Art und Steifigkeit der Befestigung des Aufnehmers am Prüfling wird an Beispielen verschiedener Meßanordnungen diskutiert und aufgezeigt.

Introduction

For accelerometers, the high frequency-response concept is rather simple and unambiguous, and most vibration engineers are familiar with the interpretation and use of the resonant curves. For force-transducers, however, the situation is not so simple on account of the two mounting surfaces. Even manufacturers seem to be confused, when stating a resonant frequency simply as

$$f = \frac{1}{2\pi} \left(\frac{k}{m + L} \right)^{1/2}$$

where k is the transducer stiffness and m and L are transducer seismic mass and specimen load-mass respectively. This frequency limit is of little significance to the customer since the frequency-response of the transducer cannot be simply derived from it. In general, the response is dependent on 1) the transducer 2) the set-up and 3) the specimen (including mounting stiffness).

Response analysis

Our experiences have shown, that a proper mechanical model for piezoelectric force transducers is a spring with a mass at each end, Fig. 1.

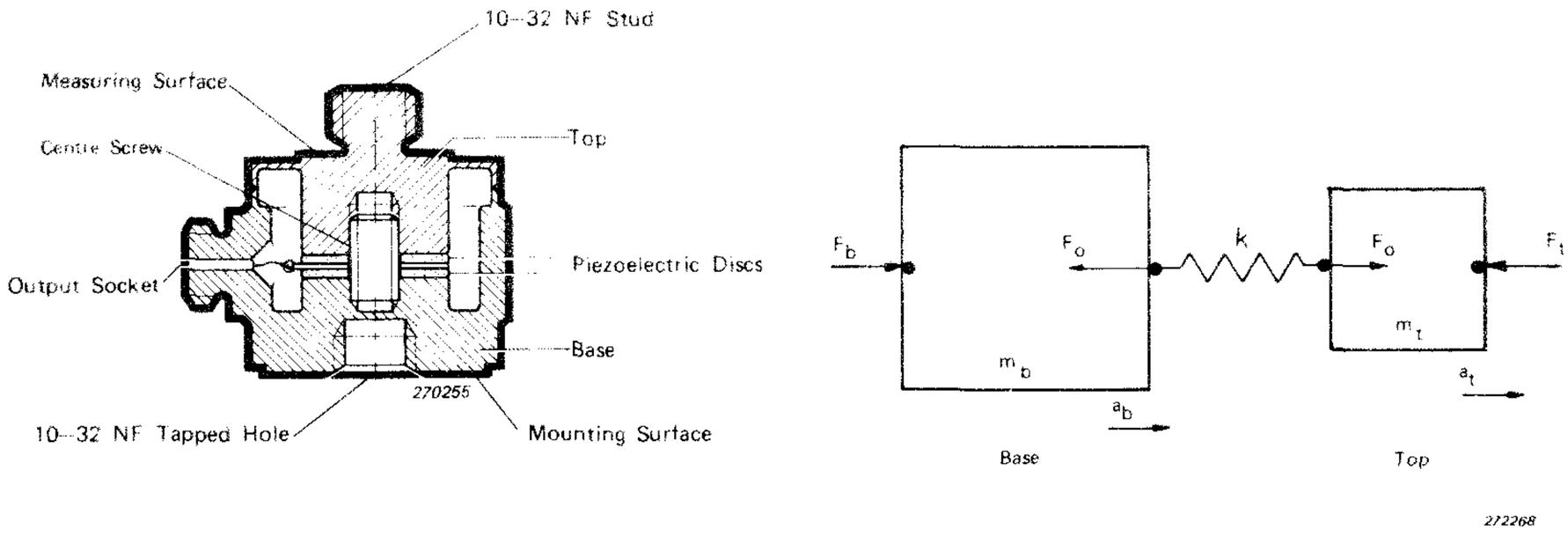

Fig. 1. Cross-sectional view of the Force Transducer and its mechanical model

In the B & K specifications for the Force-Transducers Types 8200 and 8201, the parameters k, m_b and m_t (stiffness, base-seismic mass, and top-seismic mass respectively) are stated. The electrical output from the transducer is proportional to the force F_o acting on the spring k. This is valid up to frequencies which are not too close to the acoustic resonant-frequency of the discs. This normally is in the 1 – 10 MHz range, which is far above the mechanical limit. However, the output and input forces (F_t and F_b respectively in Fig. 1) are not equal to F_o, since the seismic masses need to be accelerated. According to Newton's second law of motion.

$$F_b - F_o = m_b\, a_b \text{ and } F_o - F_t = m_t\, a_t$$

from which

$$F_o = F_b - m_b\, a_b = F_t + m_t\, a_t \qquad (1)$$

where a_b and a_t are the accelerations of the base and the top seismic masses respectively. To introduce as small an error as possible, one should always connect the end of the transducer with the smallest seismic mass to the surface, where the force is to be measured, which is assumed to be done in the following.

There are basically two types of set-ups, 1) where the specimen is excited by the force transmitted through the force transducer, and 2) where the specimen is excited by foreign forces and the force is to be measured in some suspension point.

1. Exciting force transmitted through the transducer

The set-up in Fig.2 might, for example, be part of a mechanical impedance measurement where the force F_t acting on the structure of impedance Z is to be measured. (The impedance Z should include mounting stiffness.) The force measured by the transducer is F_o (in the relevant frequency range). The transducer-frequency response is defined as

$$R = F_o/F_t = R(f) \qquad (2)$$

Using the impedance diagram in Fig.2 we obtain

$$R = F_o/F_t = 1 + \frac{j\omega m_t}{Z} \qquad (3)$$

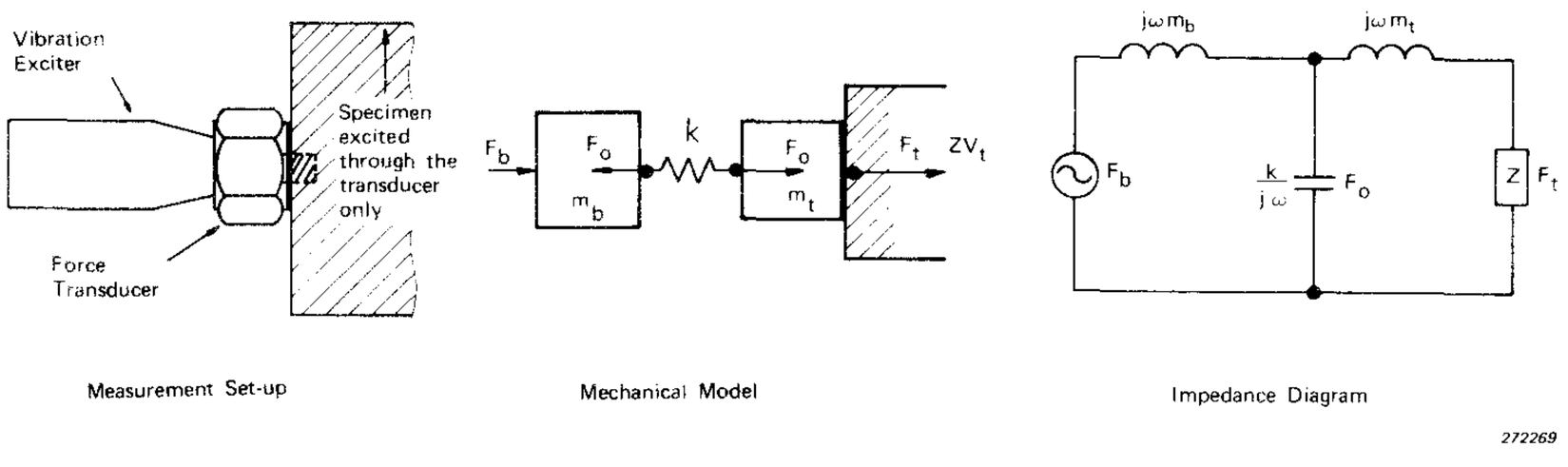

Measurement Set-up | Mechanical Model | Impedance Diagram

Fig.2. Measurement set-up Type 1

The response is *dependent* on the small seismic mass of the transducer and the impedance of the specimen, but *independent* of the heavy-base mass and the stiffness of the transducer as well as the exciter-impedance.

Note the following special cases:

a) When the impedance is a springlike structure of stiffness k_1

$$Z = k_1/j\omega$$

and

$$R = F_o/F_t = 1 - \omega^2/\left(\frac{k_1}{m_t}\right) \qquad (4)$$

which shows up as an antiresonance in the frequency response, Fig.3. The resonant frequency is determined by the small seismic mass of the transducer and the stiffness of the springlike structure.

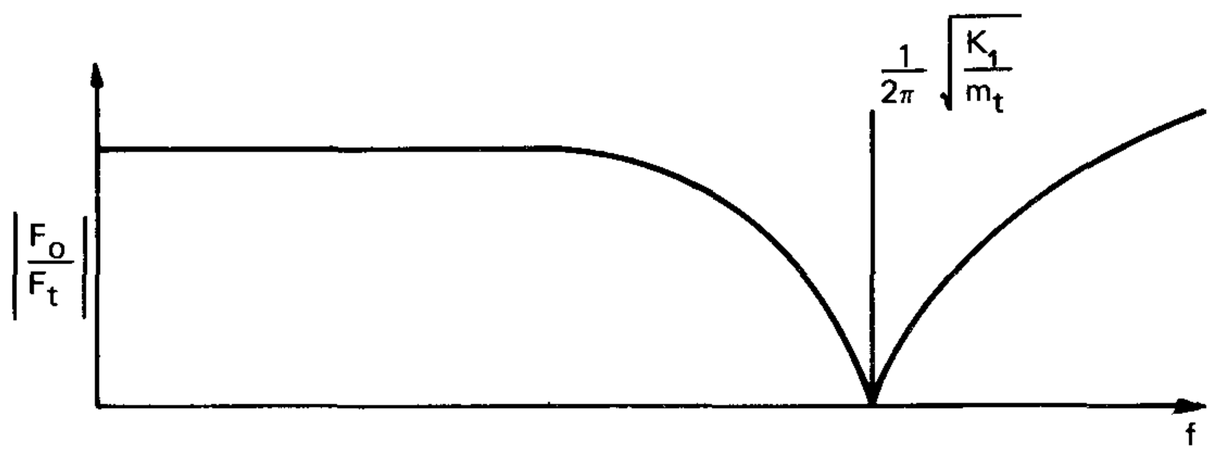

272270

Fig.3. Frequency Response for set-up Type 1a

b) When the impedance is a pure mass M

$$Z = j\omega M$$

and

$$R = F_o/F_t = 1 + \frac{m_t}{M} \qquad (5)$$

which is a frequency independent correction factor.

In point-impedance-measurements, where acceleration is measured, mass compensation is possible by electronic addition of the terms F_o and $m_t\ a_t$ (equation (1)) .

The response $\frac{F_o'}{F_t} = \frac{F_o - m_t\ a_t}{F_t} = 1$

then becomes flat at frequencies, where the compensation is true i.e. where the measured acceleration is equal to a_t.

2. Measurement of force on an excited structure by introducing a force transducer as a suspension washer

Fig.4 shows an example of such a system where, again, the measured force is F_o, but the force to be measured is F_t.

The frequency response becomes:

$$R = F_o/F_t = \frac{1}{1 + j\omega m_t/Z^*} \qquad (6)$$

$$\text{where } Z^* = \frac{k/j\omega\ (j\omega m_b + Z_f)}{k/j\omega + j\omega m_b + Z_f} \qquad (7)$$

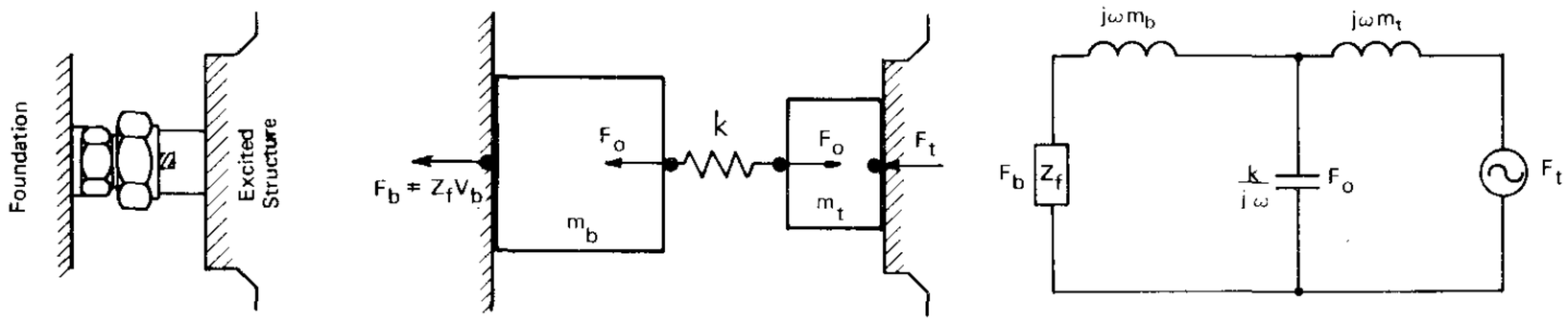

Fig.4. Measurement set-up Type 2

The foundation-impedance Z_f should include mounting-stiffness at the surface. This expression is rather complicated, however, the following special cases can be considered for clarifying the response:

a) In the case of a very heavy foundation

$$| Z_f + j\omega m_b | \gg k/\omega ,$$

and we obtain

$$R = F_o/F_t = \frac{1}{1 - \frac{\omega^2}{k/m_t}} \qquad (8)$$

which is the case of the transducer's own resonance. The resonant frequency

$$f_r = \frac{1}{2\pi}\sqrt{\frac{k}{m_t}}$$

is only dependent on the top seismic mass and the stiffness of the transducer. The response curve is shown as the upper one in Fig.5.

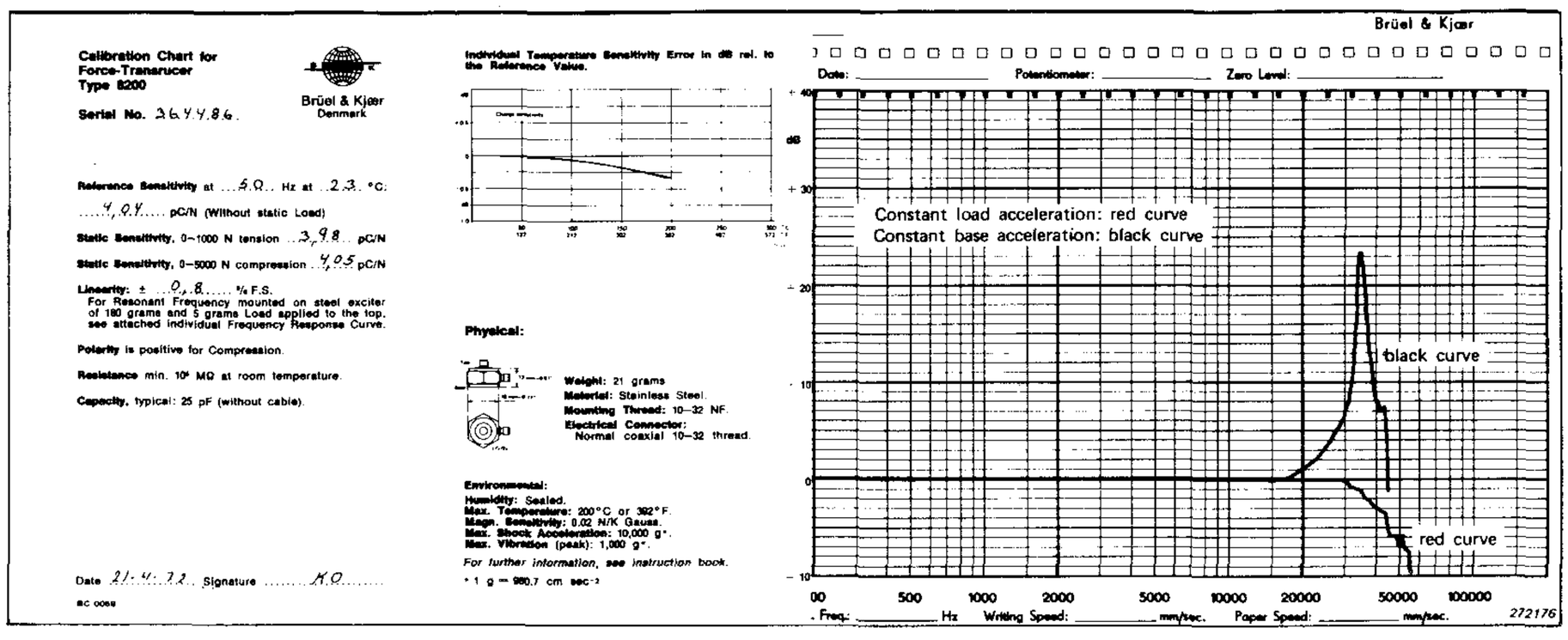

Fig.5. Frequency Response for set-up Types 1a and 2a

This curve is shown on each calibraiton chart for the force transducer Types 8200 and 8201 and is obtained by exciting the force transducer on a vibration exciter keeping the base acceleration of the transducer constant. This can be seen to correspond exactly to the case 2a) described above. The lower curve corresponds to case 1a) (see instruction manual for Force Transducer Type 8200).

b) If the foundation is compliant or the mounting to it is poor and the foundation is assumed to be spring-like of stiffness k_f the impedance would be

$$Z_f = k_f/j\omega$$

where we assume $k_f \ll k$ (k is the transducer stiffness)

For this impedance it can be shown from eq. (6) and (**7**) that the response would be

$$R = \frac{F_o}{F_t} = \frac{1 - \omega^2 \frac{m_b}{k_f}}{1 - \frac{\omega^2 (m_b + m_t)}{k_f} - \omega^2 \frac{m_t}{k} (1 - \omega^2 \frac{m_b}{k_f})} \quad (9)$$

As the term $\omega^2 \frac{m_t}{k} (1 - \omega^2 \frac{m_b}{k_f})$ is very small a resonance occurs

when $\omega^2 \approx k_f/(m_b + m_t)$.

Similarly an antiresonance occurs for $\omega^2 = k_f/m_b$.

It should be noted that since the frequencies of resonance and antiresonance are much below the resonance frequency given by eq. (8) the force transducer can in this case only be used for frequencies

$$\omega^2 < \frac{k_f}{(m_b + m_t)}$$

In this analysis the desired force is assumed to be F_t shown in Fig.4. This is true for example in a monitoring situation where the force transmitted by a machine is of interest.

3. Effects on a mechanical system by introducing a force transducer

In the above considerations the function R has been derived to determine the ratio of the measured force to the actual force. However, in some cases, the introduction of a force transducer into the mechanical system may change completely the forces existing in the system. In such cases, naturally, caution must be taken that the measurement results are only used for frequencies where the response function is flat.

The problem arises when the force transducer is introduced instead of a support member which has another stiffness than the force transducer and when both the structure and the foundation have considerably larger masses than the transducer. The most common case would be when the structure is lifted off its very stiff support to introduce one or more force transducers. Then the masses of the structure and the foundation would form a resonant system with the transducer stiffnesses which are lower than the support stiffness. The resonance frequency could be considerably lower than that existing in the normal configuration and the use of the measured data should be restricted to frequencies somewhat lower than this frequency if the task is to determine the force existing before introducing the force transducer.

When the normal support has a lower stiffness than the force transducer it would be natural to introduce the force transducer *between* the structure and the support or *between* the foundation and the support member. In these cases the total stiffness of the system is practically unchanged and the procedure outlined in section 2 could be followed. If, however, from practical reasons, compliant support members have to be *replaced* by the relatively stiff force transducers during the measurements, it is obvious that the actual force is considerably changed in the frequency range around and above the resonance frequency which exist when the compliant support is used. The measurement results could, perhaps, then be compared to for example transmissibility recordings for this arrangement.

Conclusion

High-frequency-response data for force transducers must be considered critically since the frequency response may depend not only on the force transducer and the structure on which measurements are taken but also on its foundation and support configuration. There are basically three different configurations of application of the force transducer.

1. The structure excited by a vibration exciter through the force transducer.
   The force to be measured is the point force at the transducer application point.

The frequency response depends only on the transducer top mass and the point impedance of the structure.

2. The force transmitted from the structure to the foundation through the force transducer.
   The force to be measured is the point force at the transducer application point on the structure. The frequency response depends on the transducer stiffness, the seismic masses and the point impedance of the foundation. It does not depend on the structural impedance.

3. This case is quite similar to case 2 above, except that it is important to know the force which existed before the force transducer was introduced.
   The frequency response of the measured force compared to the original force depends on the dynamic properties of the force transducer, the structure, the foundation and on the support replaced by the force transducer.

Measurement of Low Level Vibrations in Buildings

by

Torben Licht

ABSTRACT

An accelerometer with extremely high sensitivity and low impedance output has been developed. The application of this accelerometer in the analysis of low-level building vibrations has been studied. Measurements on different structures will be presented.

SOMMAIRE

Un accéléromètre à sensibilité extrêmement élevée et à sortie basse impédance a été développé. On a étudié les applications de cet accéléromètre pour l'analyse des vibrations de faibles niveaux dans les immeubles. Cet article présente des mesures effectuées sur différentes structures.

ZUSAMMENFASSUNG

Bei Brüel & Kjær wurde ein neuer Beschleunigungsaufnehmer mit extrem hoher Empfindlichkeit (Übertragungsfaktor) und niedriger Ausgangsimpedanz entwickelt. Die Verwendung dieses Aufnehmers für die Analyse niedriger Schwingungspegel an Gebäuden wurde untersucht. Messungen an unterschiedlichen Strukturen werden besprochen und die Meßergebnisse gezeigt.

Introduction

In the last decade extensive use has been made of piezoelectric accelerometers for vibration measurements. Most types of applications have concerned vibration levels from 0.1 to 1000 g in the 1 to 5000 Hz frequency range. However, in the last few years there has been an increasing demand for piezoelectric accelerometers which are suitable for vibration measurements on large structures such as buildings and ships, etc. In these applications the vibration level is usually below 1 g and the frequency range is from 1 to 1000 Hz, consequently the weight of the accelerometer is of little importance.

To comply with these demands an accelerometer with integral preamplifier and very high sensitivity has been developed. A measuring system which makes use of this accelerometer for mechanical impedance measurements on a large concrete beam in a building is described below.

---

*) Paper presented at the 7th International Congress on Acoustics, Budapest, Hungary. 18 – 26. August 1971.

Measuring System

A schematic diagram of the newly developed accelerometer used in the measuring system is shown in Fig. 1, while its most important characteristics are summarized in Table 1.

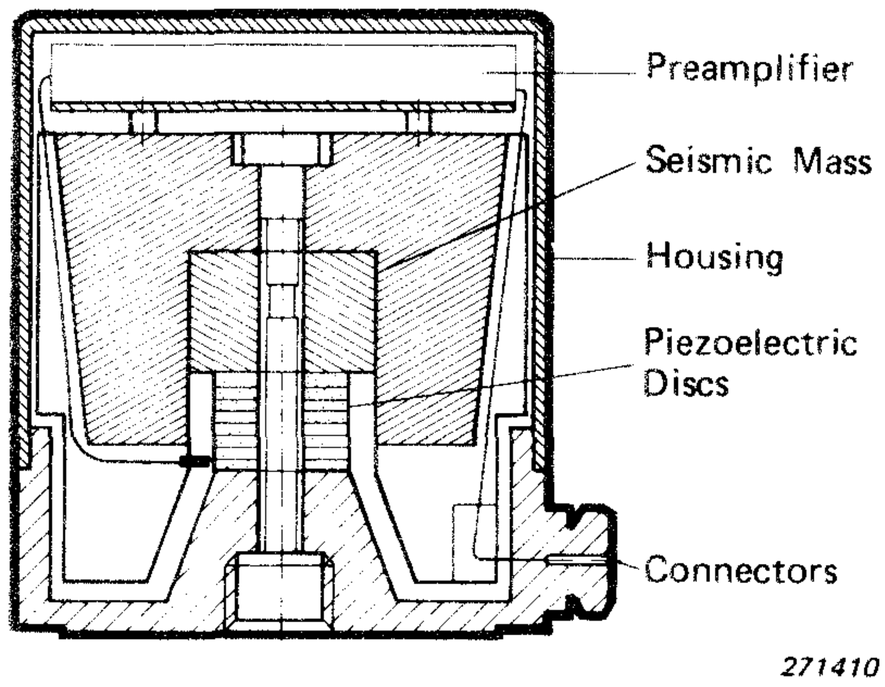

Fig. 1. Schematic diagram of high sensitivity accelerometer

Accelerometer sensitivity	10.0 + 0.2 V/g
Accelerometer mounted resonance	2500 Hz
Preamplifier gain	approx. 0 dB
Preamplifier output impedance	$<500\ \Omega$
Preamplifier max. output current	1.4 mA
Preamplifier max. output voltage	10 V
Frequency response (acc. + preampl.) (10% limits)	0.2 – 1000 Hz
Noise Level (2 – 1000 Hz)	$<40\ \mu V$
Maximum temperature transient sensitivity (3 Hz LLF)	4×10^{-5} g/°C
Special connector gives charge output via	1000 pF
Power Supply	2 mA, 28 V DC
Weight	approx. 600 g

Table 1. Accelerometer specifications

The sensitivity of the accelerometer is about 100 to 1000 times that of most ordinary types of accelerometers. The noise level of the preamplifier is 5 to 10 times more than conventional preamplifiers because of a special filtering arrangement. Consequently the minimum vibration level that can be measured with the accelerometer is approximately 10 μg which is about the same order of magnitude as the background vibrations in quiet areas, free from the influence of traffic vibrations and other disturbances.

The mechanical impedance measurement system in which the accelerometer was used is shown in Fig.2. The shaker is mechanically coupled to a force transducer via a ball joint and a push rod. The force transducer transfers the force from the shaker to the concrete beam via a stainless steel plate. Using wax the accelerometer is mounted as close as possible to the force transducer.

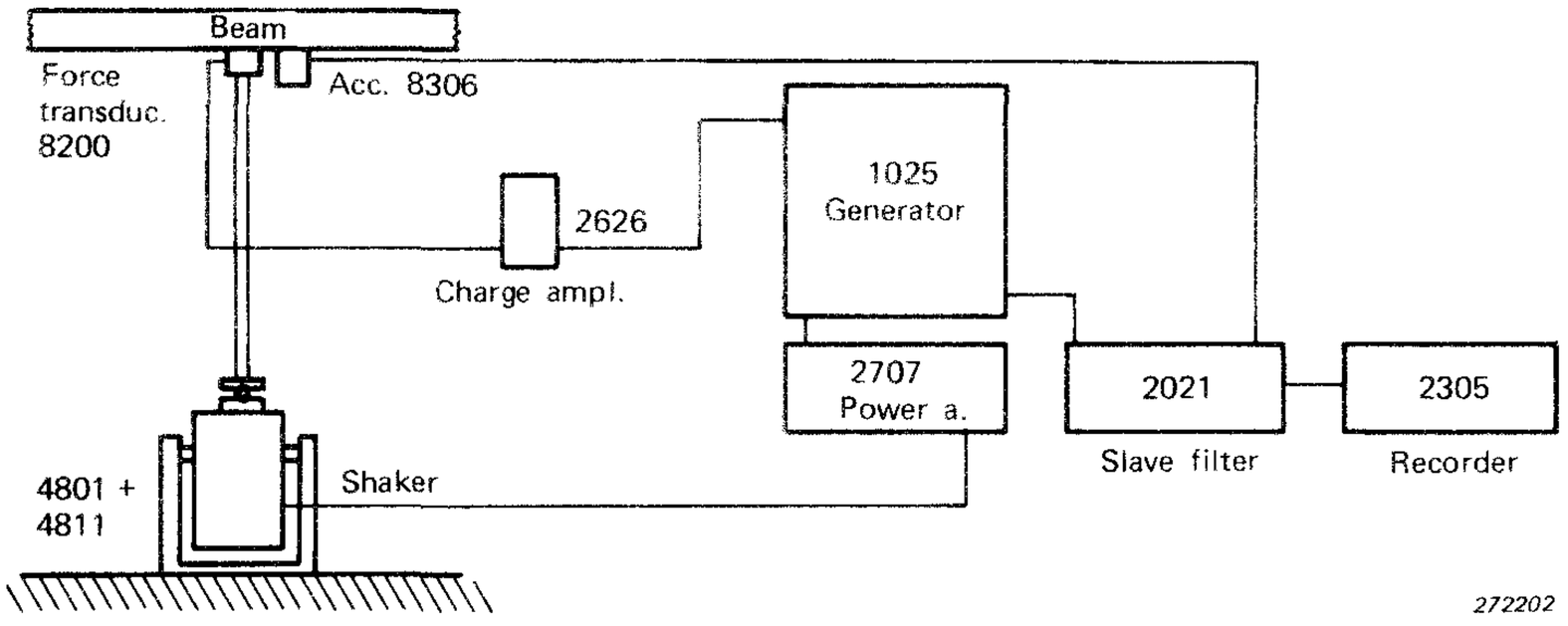

Fig.2. Mechanical impedance measurement system

The force applied to the beam is kept constant (or on a line of constant slope) by amplifying the output from the force transducer using a Charge Amplifier Type 2626 and applying it to the compressor facility of the Automatic Exciter Vibration Control Type 1025. The signal from the 1025 is fed to a Power Amplifier Type 2707 which drives the moving coil of the shaker. The 2707 also provides a dc current to the coil to give a preload force of 15 kp.

The high frequency output (25 – 30 kHz) from the 1025 is used to synchronize the Heterodyne Slave Filter Type 2021 allowing it to follow the shaker vibration frequency so that only the output from the accelerometer at the excitation frequency is amplified and recorded by the Level Recorder Type 2305.

Recording and Calculation. Fundamental Mode:
The most convenient parameter to record was the so-called mechanical driving point mobility which is defined as:

$$M = \frac{V}{F}$$

where V is the velocity of the point when a force F is applied at that point. Normally complex notation is used, but in this case only the numerical value of M is recorded.

Since velocity is obtained by integration of the acceleration signal,

$$v = \frac{a}{\omega} \quad \text{and} \quad M = \frac{a}{\omega F}$$

for sinusoidal excitation.

Thus it can be seen that if the acceleration of the beam is measured, keeping ωF constant while sweeping over the frequency range, a plot of the mobility curve is obtained. In practice this is obtained by feeding the force signal of the servo-loop to the velocity generator input of the Exciter Control Type 1025.

Fig.3 shows one of the recordings obtained. The maximum applied force force was 8.5 kp peak at 10 Hz decreasing at a rate of 6 dB/octave as the frequency was scanned. The two straight lines drawn on the measured mobility curve correspond to the mobility of an ideal spring ($M = j\omega/k$) and the mobility of an ideal mass ($M = 1/j\omega m$). These lines show that from 10 Hz upto approximately 40 Hz the beam moves as a spring with certain resonances, while from 40 Hz to 200 Hz and above it moves like a mass.

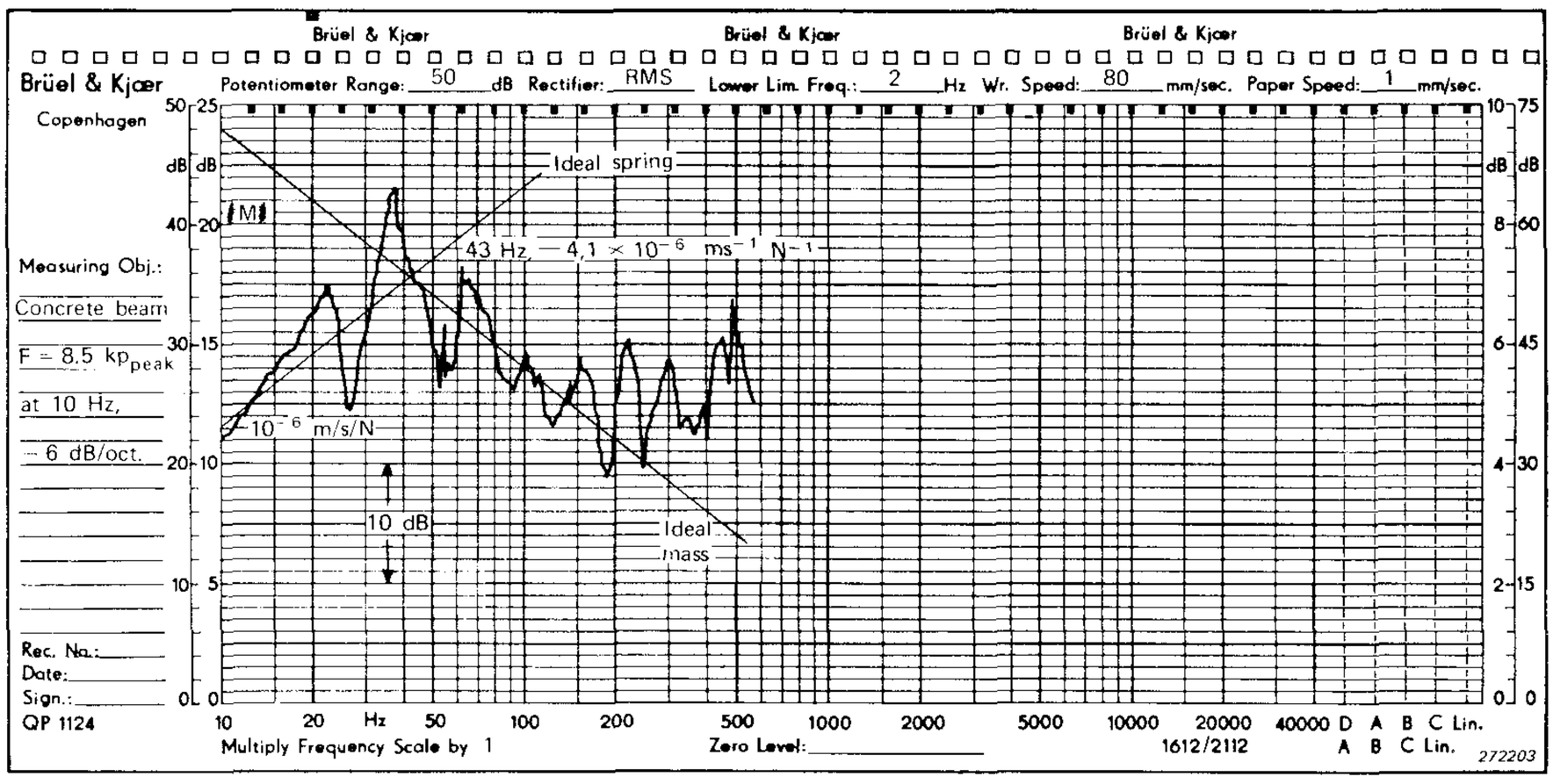

Fig.3. A mobility recording

Fig.4 shows the mobility of a simple system consisting of a mass suspended by a spring. By comparing the curves in Figs.3 and 4 we can conclude that as a first approximation the beam also behaves like the system shown in Fig.4.

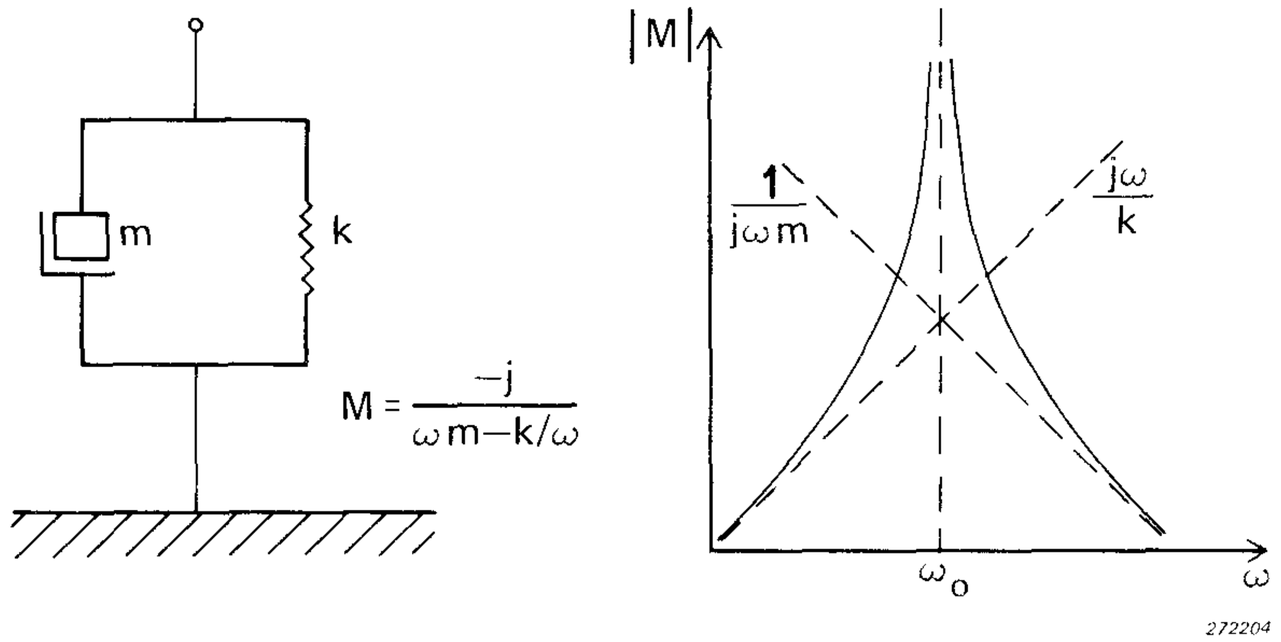

Fig.4. Mass loaded spring and its mobility response

At the point where the two lines intersect

$$|M| = \frac{1}{\omega m} = \frac{\omega}{k}$$

Taking the value of mobility ($4 \cdot 1 \times 10^{-6}$ ms^{-1}/N) and frequency (43 Hz) at this point, the mass and the stiffness of the beam can be evaluated and are shown in Table 2. Also shown are the values for hinged-hinged and clamped-clamped beams, which were calculated using standard formulae.

	Measured values	Beam aline		Beam + concrete floor	
		hinged-hinged	clamped-clamped	hinged-hinged	clamped-clamped
K/(10^6 kp/m)	6.7	3.24	13.0	3.50	14.0
m/(kg)	900	560	410	1180	866

Table 2. Calculated values

The dimensions used are shown in Fig.5 while the constants for concrete are

$$E = 0.3 \cdot 10^6 \text{ kp/cm}^2 \text{ and } \sigma = 2.4 \cdot 10^{-3} \text{ kg/cm}^3$$

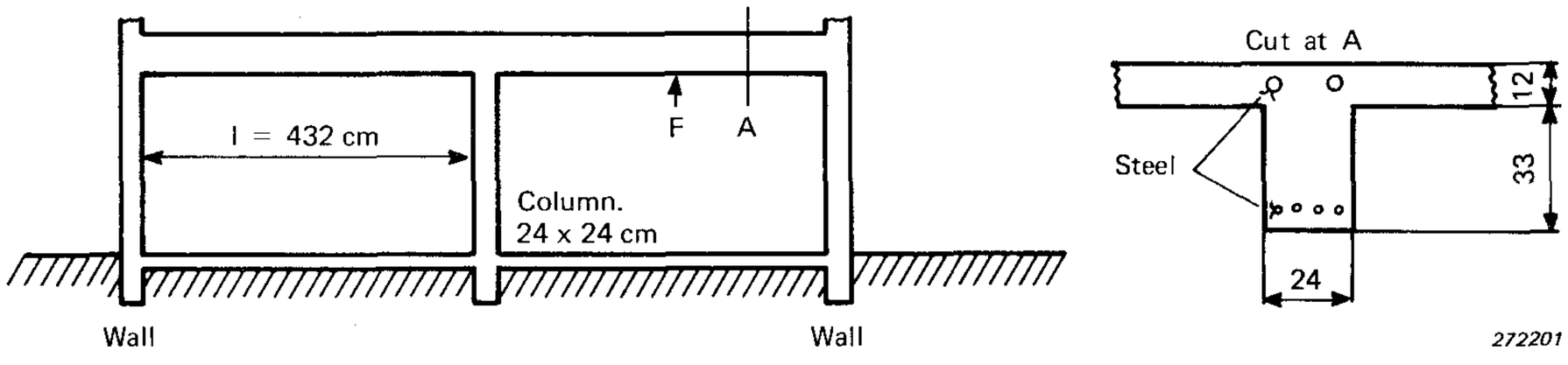

Fig.5. Dimensions of the structure

Since the beam carries a 12 cm thick floor, it is unrealistic to use the weight of the beam alone and therefore the last two columns of Table 2 give the values for k and m when the mass and stiffness of part of the floor (50 cm on either side of the beam) is added.

More sophisticated calculations could be made on the structure if all dimensions and loadings were known, but as the purpose was mainly to show the possibilities of the instrumentation and not to obtain real values for the building, this has not been done.

It can be seen from Table 2 that the values calculated for the concrete beam and the floor are in good agreement with the measured results, since we must expect the results to lie between the Hinged-Hinged and Clamped-Clamped cases.

Higher Resonances

Fig.3 shows that, apart from the fundamental mode which gives a mobility peak and a change in slope, there are several other resonances. From Fig.5 it has to be expected that the beam is in fact twice as long as the part on which we made the first calculations. A system which is expected to be a good model of this is shown in Fig.6.

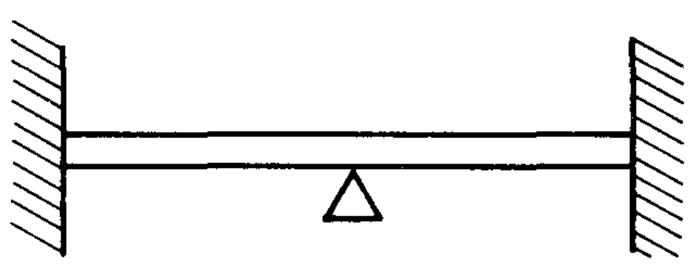

272200

Fig.6. Clamped- hinged-clamped beam

From this system the frequencies for the different modes have been calculated (lit. 1, p. 7-21). The fundamental mode for half of the beam corre-

sponds to the second mode. By scaling the frequencies so that the second mode frequency is equal to the measured frequency of 36 Hz we can find for the first five modes the ratio of the calculated values to the measured values. The results are shown in Table 3.

Mode	1	2	3	4	5
f meas./(Hz)	22	36	70	95	160
f calc./(Hz)	25	36	80	99	167
ratio $\frac{fc}{fm}$	1.14	1.00	1.14	1.04	1.04

Table 3. The ratios of calculated to measured frequencies

It can be seen that the agreement between the measured and calculated values is good, especially when it is remembered that the applied model is quite simple.

Other Measurements

After the mobility measurements, the acceleration transmitted from a big plate cutting machine was measured at the same position. The signal was amplified by a Charge Amplifier Type 2626 and recorded using the FM Tape Recorder Type 7001. After a frequency transformation the maximum value for one cut of the machine was analyzed and stored by the Real Time Analyzer Type 3347. By comparing the results from an analog measurement made near the machine, it was concluded that the concrete construction acts as a filter, transmitting most of the frequencies where the mobility is high.

Conclusion

The measurements have shown that the high sensitivity accelerometer is an excellent tool for the study of low level building vibrations. The mobility measurements show a good agreement with the calculated values and it is believed that the method can be used as a non-destructive test in the control of building quality. It should also be possible to use the method for initial tests on the ability of a building to transmit noise from one part of its structure to another.

Literature

C.M. HARRIS and C.F. CREDE: Shock and Vibration Handbook. McGraw-Hill, 1961.

Brief Communications

The intention of this section in the B & K Technical Reviews is to cover more practical aspects of the use of Brüel & Kjær instruments. It is meant to be an "open forum" for communication between the readers of the Review and our development and application laboratories. We therefore invite you to contribute to this communication whenever you have solved a measurement problem that you think may be of general interest to users of B & K equipment. The only restriction to contributions is that they should be as short as possible and preferably no longer than 3 typewritten pages (A4).

Measurement of Damping Factor using the Resonance Method

Complement to the Measurement of the Complex Modulus of Elasticity

by

*Andràs Kelemen, dipl.phys. *)*

At a resonant peak the damping factor (d) is given by

$$d = \Delta f / f_o$$

Δf is the bandwidth at the half power points.
f_o is the resonant frequency.

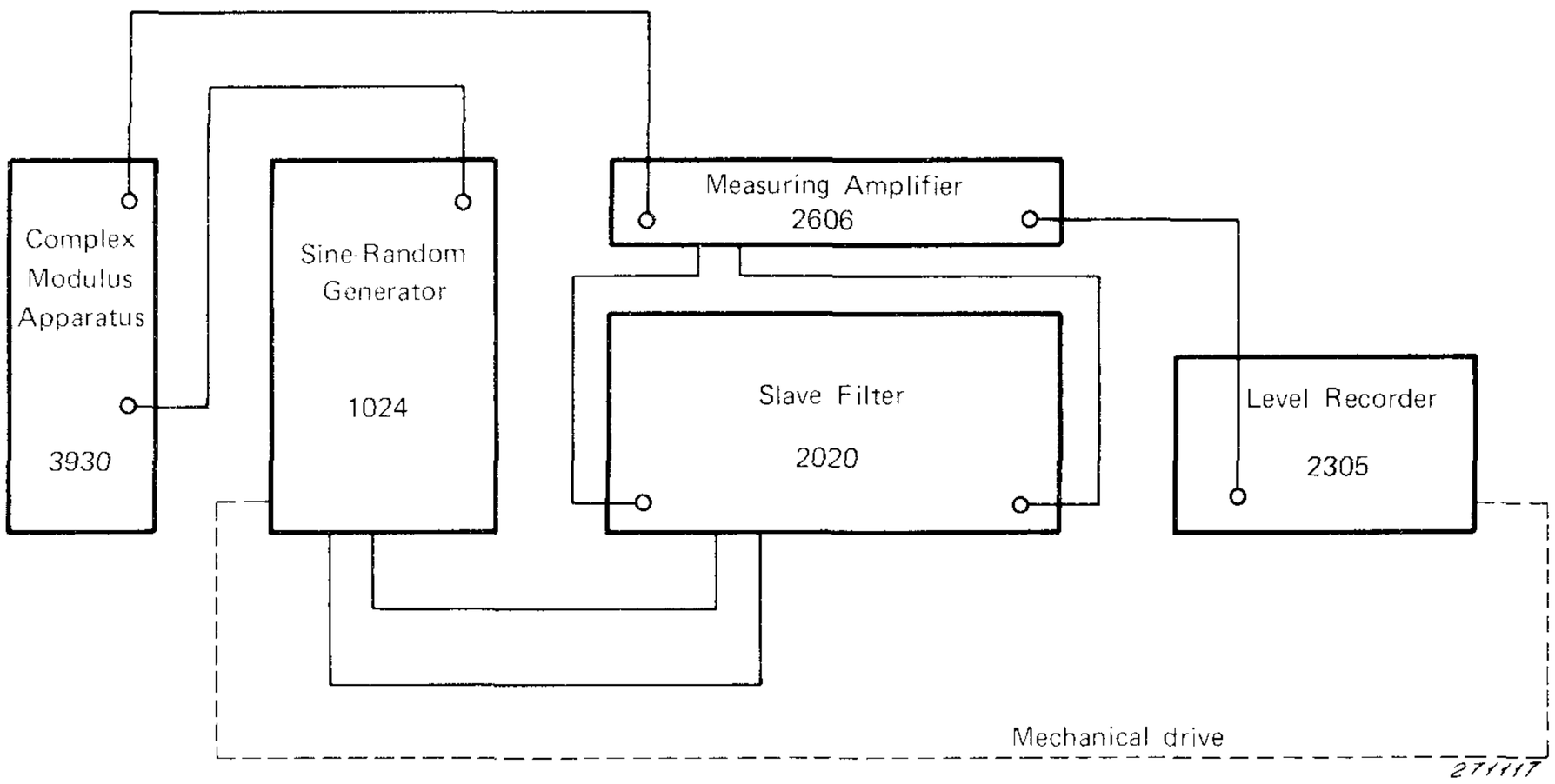

Fig. 1. Block Diagram

---

*) Acoustical Research Laboratory, Electroacoustical Factory, Budapest, Hungary.

A block diagram of the instrumentation used is shown in Figure 1. If the generator and level recorder scan rates are equal the resulting amplitude-frequency characteristic (Fig.2) is such that the measurement of the half power bandwidth of any resonant peak is limited in accuracy. The resonant peak can be "stretched", and Δf therefore determined more exactly, by driving the generator from Drive shaft II of the level recorder and choosing the paper speed accordingly. However, evaluation of Δf is still difficult and at high frequencies accuracy is further reduced since the frequency scale is logarithmic.

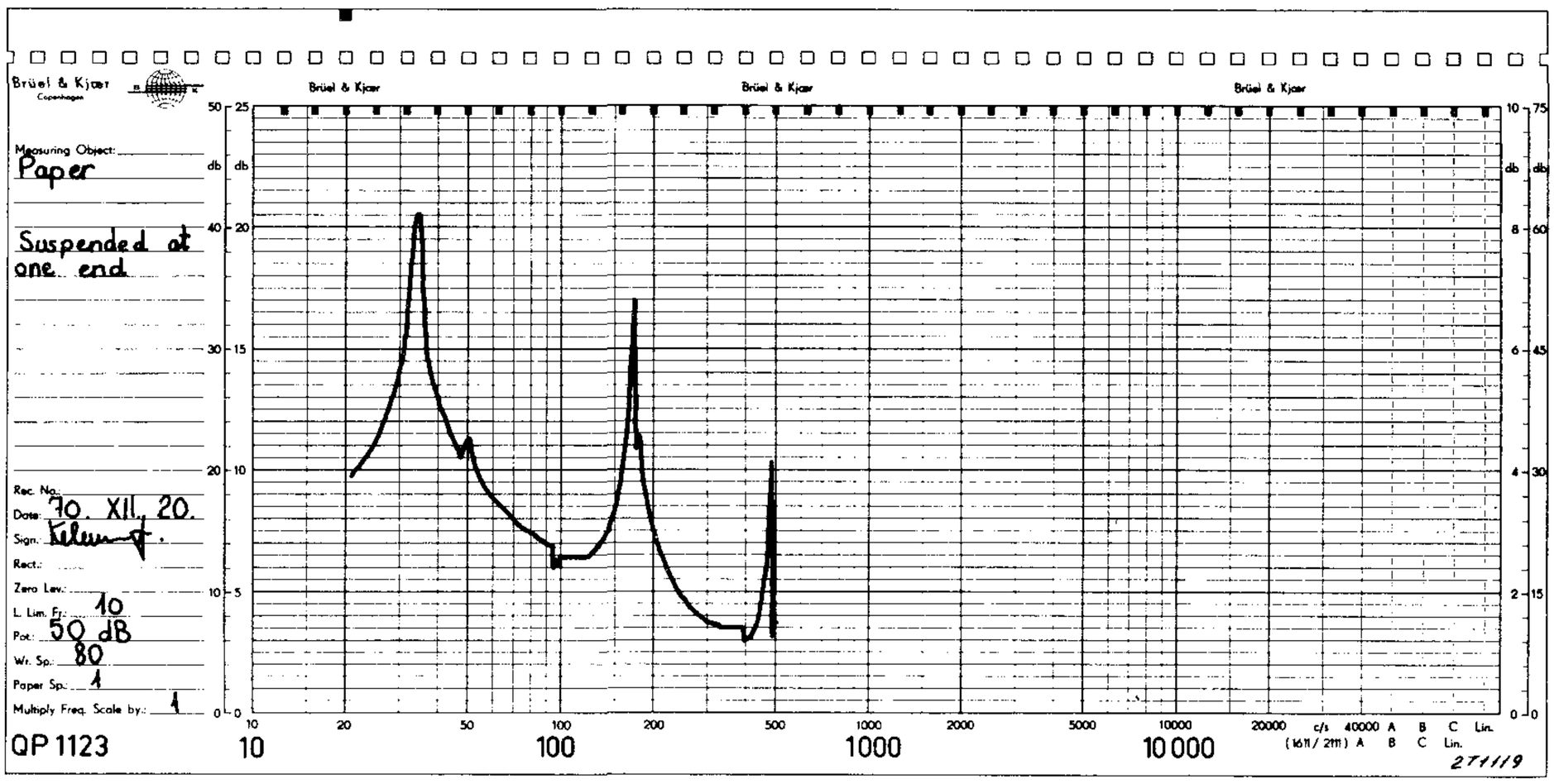

Fig.2. Recorded vibration response of a paper sample bar.

A much more exact measurement of Δf can be made if the frequency of the generator is changed linearly. This can be done using the Frequency Increment control to vary the generator frequency as the resonant peak is recorded. (The approximate resonant frequency has to be first set-up on the logarithmic scale). The Frequency Increment control spans ± 50 Hz either side of nominal and this is in excess of the half power bandwidth of the resonant peaks due to ordinary materials.

In practice this measurement technique was implemented by connecting Drive Shaft II of the Level Recorder rigidly to the shaft of the Frequency Increment capacitor of the generator. Cam operated micro-switches (normally open) were fitted and arranged to close at the extremes of shaft rotation, switching off the drive and thus preventing damage to the generator or Level Recorder. The electrical connections are given in Fig.3.

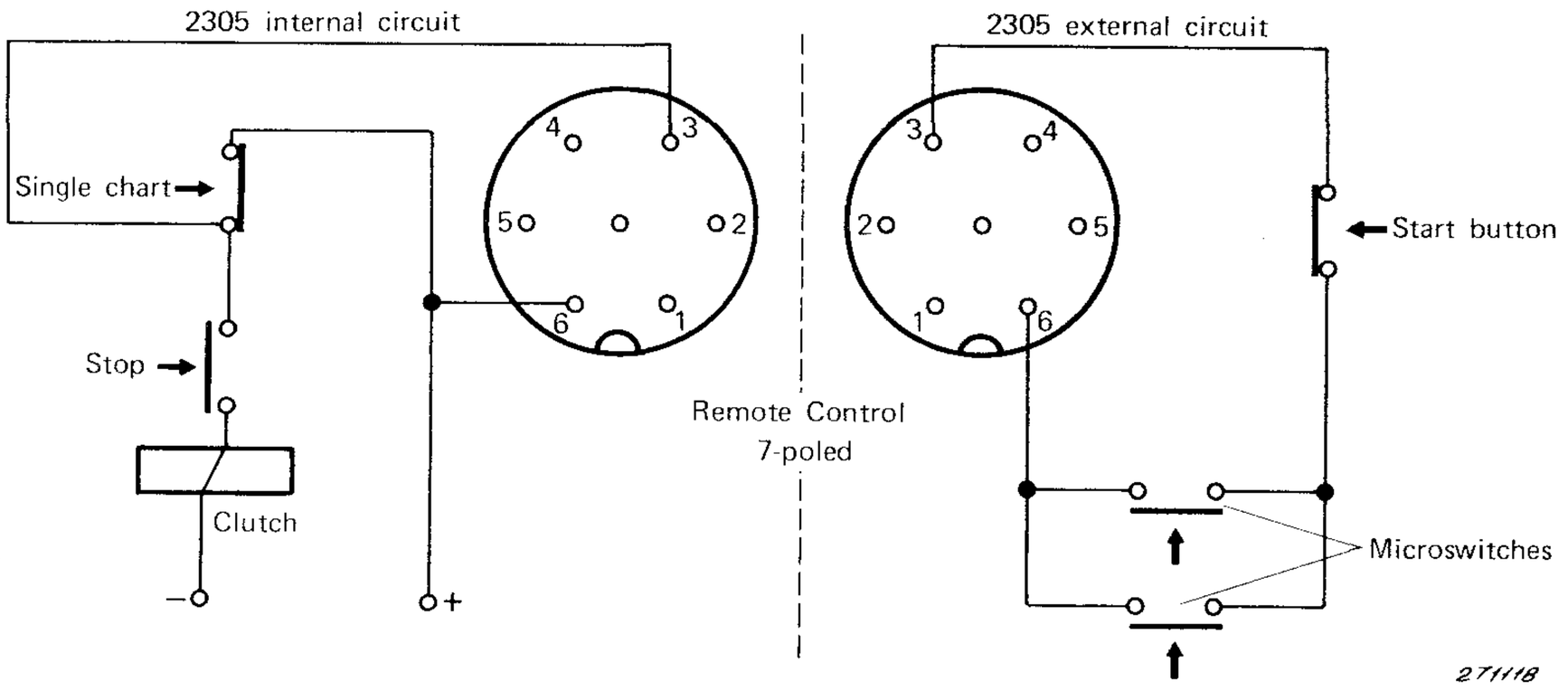

Fig.3. Circuit Diagram

To record a resonance first set the generator to the approximate resonant frequency f_o and the Level Recorder to Continuous Recording with the Motor switch at Stop. The cam should be set at one extreme thus holding one of the micro-switches closed. To commence sweeping the Level Recorder clutch must be energized by pressing the external Start Button.

This can be released as soon as the cam has turned sufficiently to open the micro-switch. The sweep continues until the cam closes the second micro-switch.

To assist in the evaluation of curves produced the template (Fig.4) was designed. It consists of two horizontal parallel straight lines, with the lower line graduated linearly in frequency. To use the template lay it over the

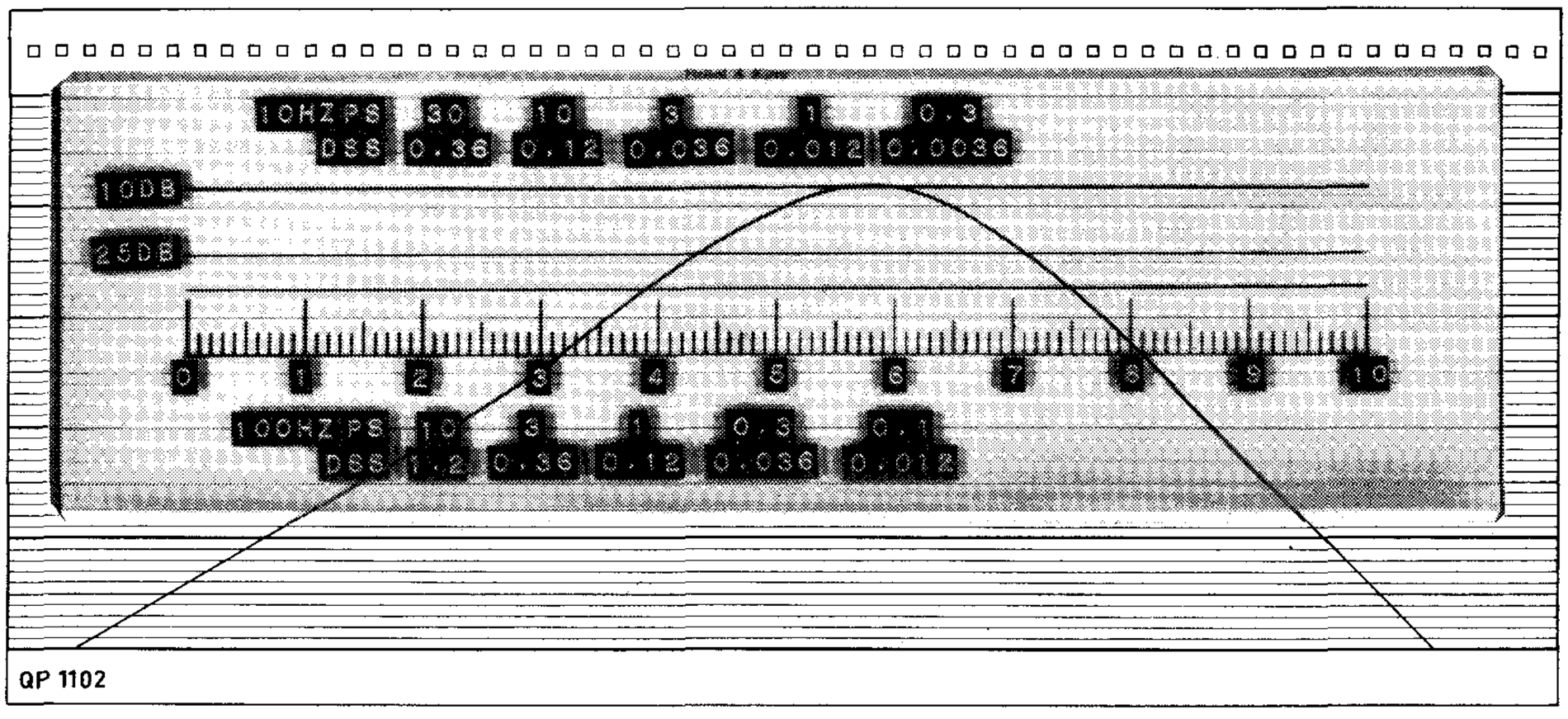

Fig.4. Illustration of the use of the template

resonant curve with the upper line set to the peak. The half power band width can be read off directly on the lower line. This template can also be used for other paper and drive shaft speeds depending on their ratio. The template is also constrained by the Range Potentiometer used.

To summarize, a complete set of measurements is made by initially recording the overall amplitude-frequency characteristic with the flexible shaft connected to Drive Shaft I. Drive Shaft II must be dis-engaged during this recording by lifting the Drive Shaft Speed Control on the Level Recorder. The approximate resonant frequencies are noted and one is set up on the generator Frequency Control.

The resonant curve is then recorded as previously detailed and analyzed with aid of the template.

Low Frequency Charge Amplifier Type 2628

The Low Frequency Charge Amplifier Type 2628, as the name itself suggests, is developed for handling very low frequency acceleration signals and quasi-static signals as those encountered in short-term static force measurements. Other application of the instrument would be in the measurement of long duration shocks. Depending on the gain setting it has time constants of upto 100.000 seconds corresponding to a low frequency limit of 2 μHz. A three digit sensitivity adjustment conditions the amplifier to the exact sensitivity of the transducer, facilitating calibration of the system especially when transducers of different sensitivities are used. Depending on the transducer sensitivity the output of the preamplifier can be chosen in steps from 0.1 mV/unit to 10 V/unit. The time constant of the input stage can be adjusted in four steps between 100.000 seconds and 0.05 seconds corresponding to 3 dB cut off frequencies of 2 μHz to 3 Hz. The circuit is cleared by a manual reset or from a remote switch or logic circuit connected to a socket on the rear panel. A low pass filter is incorporated to obtain upper limiting frequencies in steps, between 100 Hz and 100 kHz. Two signal level indicators are provided, one to indicate overload and the other to indicate when the output is within 20 dB of full output, yielding best signal to noise ratio.

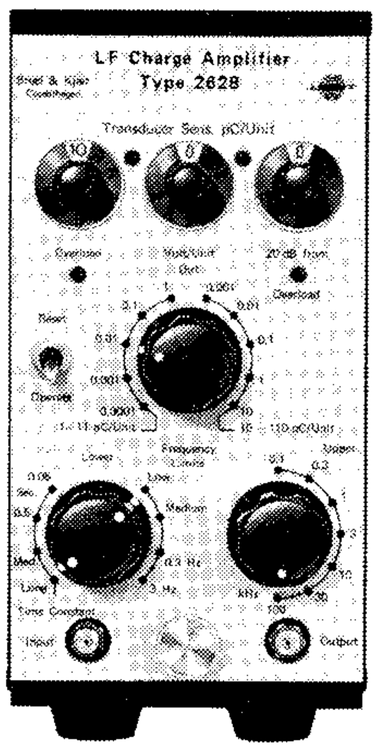

Subminiature Accelerometer Type 8307

Vibration measurements on thin skins and membranes, such as those encountered in air craft and car shells, require extremely lighweight accelerometers, as the weight of the transducer would tend to change the mode of vibration. The Subminiature Accelerometer Type 8307 weighing only 0.4 grams satisfies this need, and is also useful for complex structures where the accelerometer must be sited in a confined space. To minimise acceler-

ometer responses due to cable movement, a low noise teflon cable is rigidly bonded to the Beryllium base of the accelerometer. Relative to the size of the accelerometer, both the charge and voltage sensitivities are high. The resonant frequency of the accelerometer is 75 kHz permitting operation upto 25 kHz within the + 10% sensitivity deviation level.

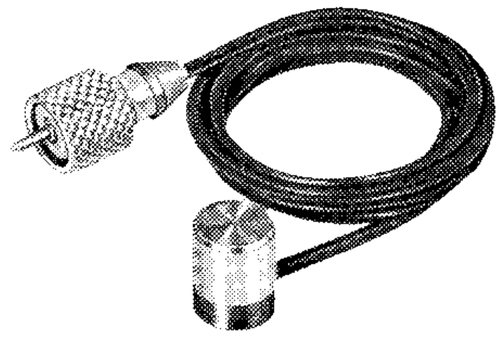

Shock Accelerometer Type 8309

An addition in our series of accelerometers is the Shock Accelerometer Type 8309, particularly developed for measurement and analysis of high level transient vibrations and shocks, as well as very short duration impulses. With its high resonant frequency of 180 kHz the accelerometer is well suited for tests on pneumatic impact tools such as rock drills, shock measurements on valves of internal combustion engines, and shocks due to explosions. The transducer's rugged construction ensures reliable operation under the severe conditions imposed by such environments. Additionally the integral cable construction reduces the size and weight of accelerometer as well as increses reliability at shock levels as high as 100.000 g. The rather high transverse resonance frequency is a particularly attractive feature in high level shock measurement, where the cross motion of a test object is often difficult to define. Zero shift introduced in the output by high level shocks has been reduced to negligible proportions by careful treatment of the piezoelectric discs. The integral treated fixing stud is adequately dimensioned to transmit the motion of the test point to the piezoelectric element without distortion.

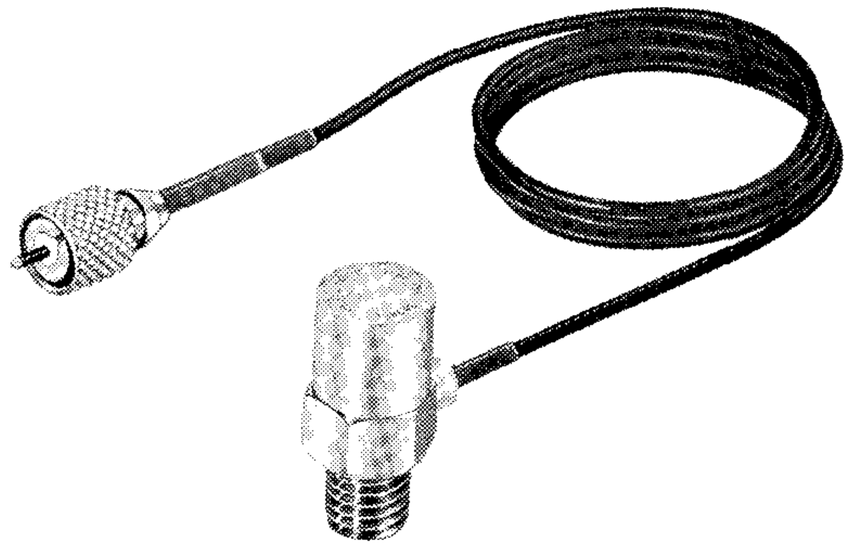

PREVIOUSLY ISSUED NUMBERS OF BRÜEL & KJÆR TECHNICAL REVIEW

(Continued from cover page 2)

Accelerometer Configurations.
Vibration Monitoring and Warning Systems.

1–1969 The Use of Digital Systems in Acoustical Measurements.
Impulse Noise Measurements.
Low Frequency Measurements Using Capacitive Transducers.
Details in the Construction of a Piezo-electric Microphone.
A New Method in Stroboscopy.

4–1968 On the Damaging Effects of Vibration.
Cross Spectral Density Measurements with Brüel & Kjær Instruments. (Part II).

3–1968 On the Measurement and Interpretation of Cross-Power-Spectra.
Cross Power Spectral Density Measurements with Brüel & Kjær Instruments (Part 1).

2–1968 The Anechoic Chambers at the Technical University of Denmark.

1–1968 Peak Distribution Effects in Random Load Fatigue.

4–1967 Changing the Noise Spectrum of Pulse Jet Engines.
On the Averaging Time of Level Recorders.

3–1967 Vibration Testing – The Reasons and the Means.

2–1967 Mechanical Failure Forecast by Vibration Analysis.
Tapping Machines for Measuring Impact Sound Transmission.

1–1967 FM Tape Recording.
Vibration Measurements at the Technical University of Denmark.

SPECIAL TECHNICAL LITERATURE

As shown on the back cover page Brüel & Kjær publish a variety of technical literature which can be obtained free of charge.
The following literature is presently available:

Mechanical Vibration and Shock Measurements (English, German)
Acoustic Noise Measurements (English),) 2. edition
Architectural Acoustics (English)
Power Spectral Density Measurements and Frequency Analysis (English)
Standards, formulae and charts (English)
Instruction manuals (English, some available in German, French, Russian)
Catalogs (several languages)
Product Data Sheets (English, German, French, Russian)

Furthermore, back copies of the Technical Review can be supplied as shown in the list above. Older issues may be obtained provided they are still in stock.

PRINTED IN DENMARK • K. LARSEN & SØN A/S • 2860 SØBORG

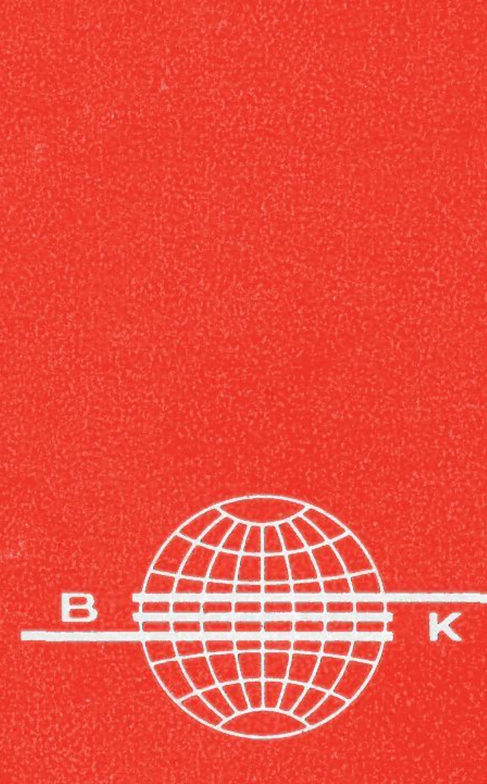

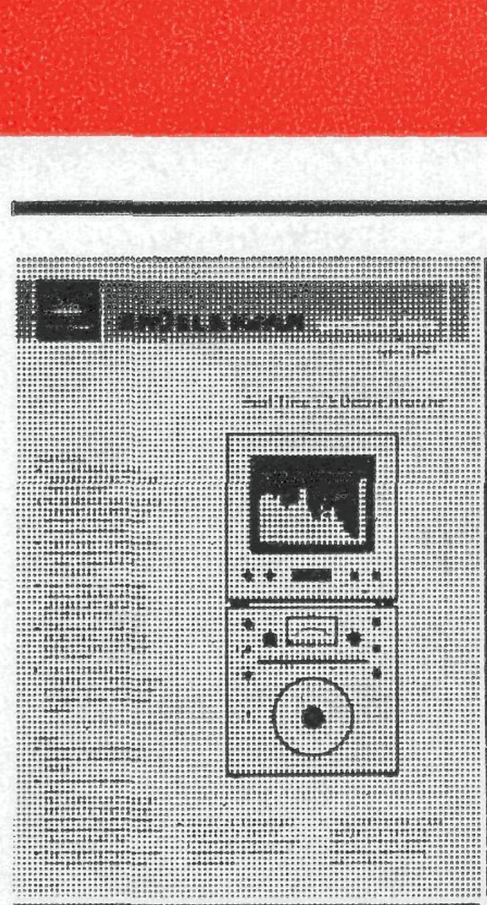

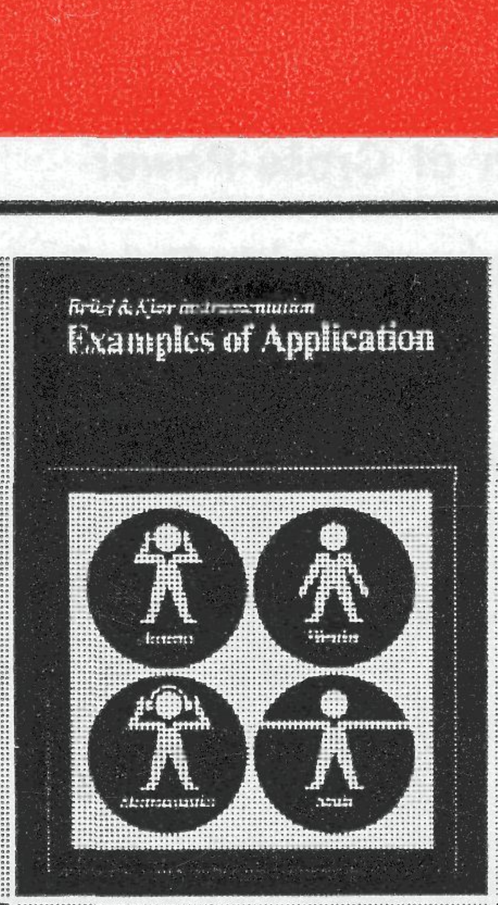

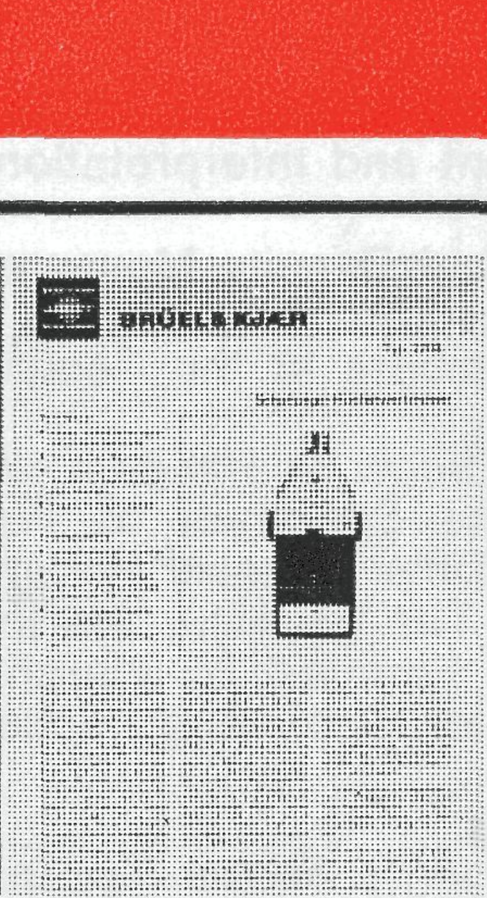

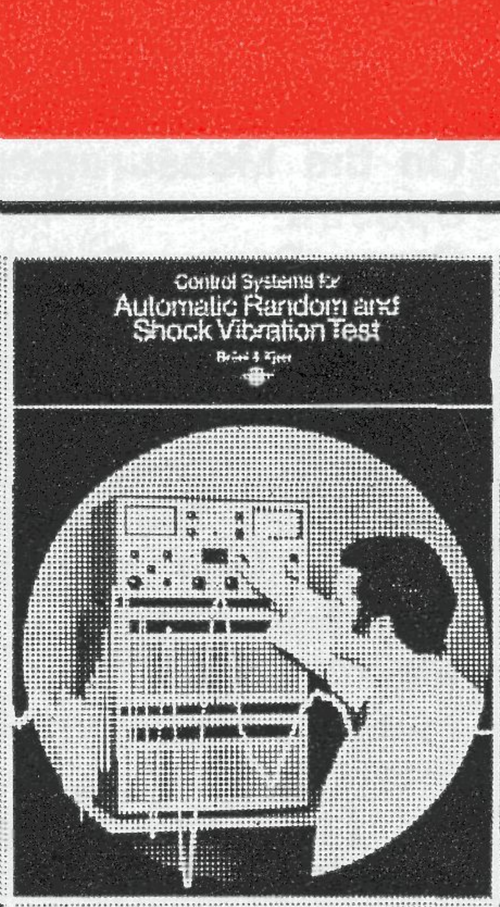

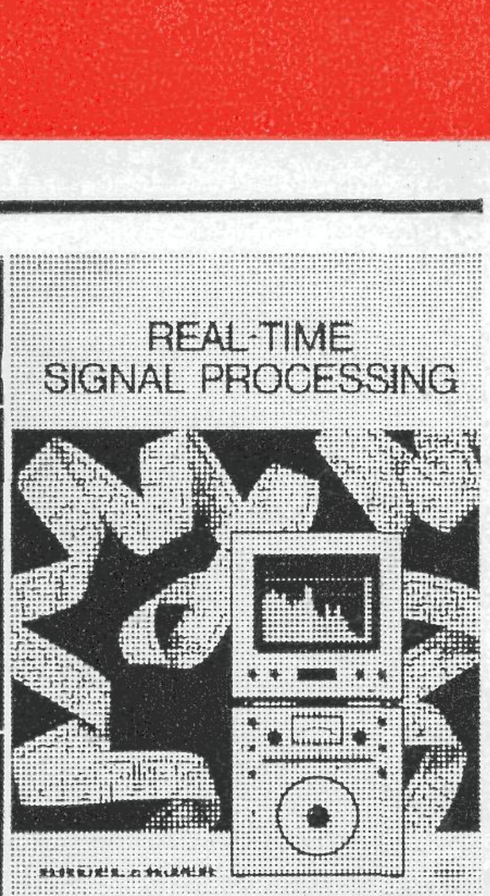

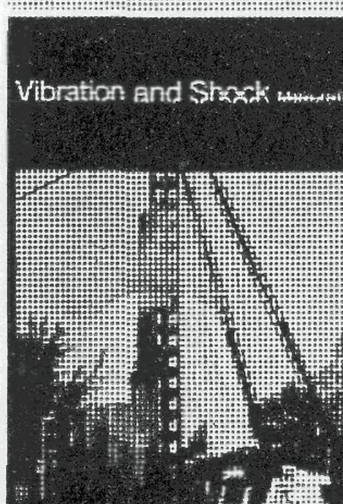

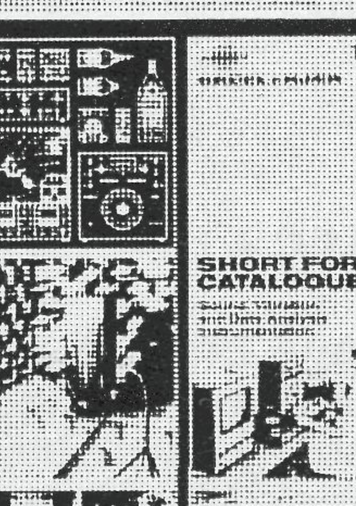

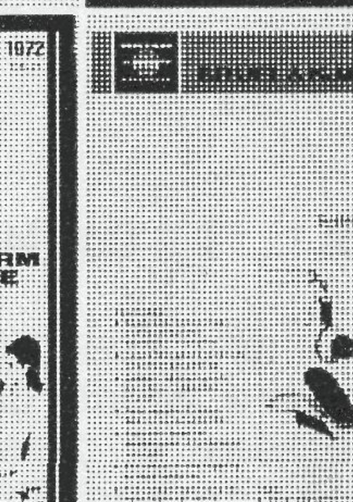

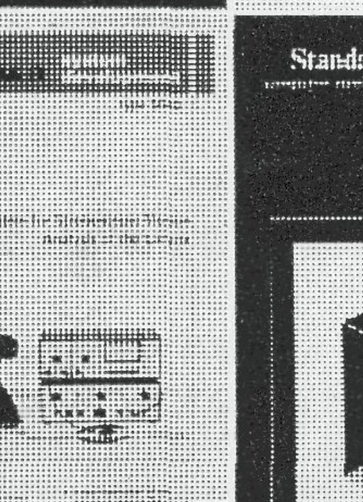

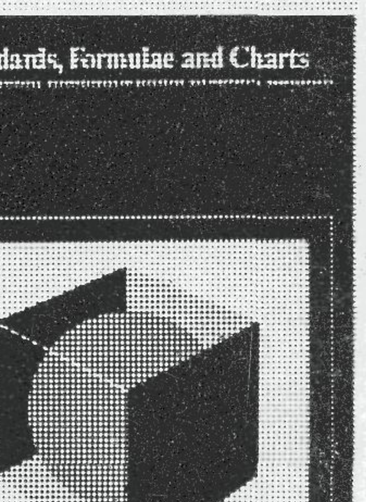

BRÜEL & KJÆR
DK-2850 Nærum, Denmark. Teleph.: (01) 80 05 00. Cable: BRUKJA, Copenhagen. Telex: 15316